Progress with the Finite-Volume Module of the IFS

Christian Kühnlein, Sylvie Malardel, Piotr Smolarkiewicz,...

$$\frac{\partial \mathcal{G}\rho}{\partial t} + \nabla \cdot (\mathbf{v}\mathcal{G}\rho) = 0$$

$$\frac{\partial \mathcal{G}\rho\mathbf{u}}{\partial t} + \nabla \cdot (\mathbf{v}\mathcal{G}\rho\mathbf{u}) = \mathcal{G}\rho\left(-\Theta_d \widetilde{\mathbf{G}}\nabla\varphi' - \frac{\mathrm{g}}{\theta_a}(\theta' + \theta_a(\epsilon q_v' - q_l - q_r)) - \mathrm{f}\times\left(\mathbf{u} - \frac{\theta}{\theta_a}\mathbf{u}_a\right) + \mathrm{M}(\mathbf{u}) + \mathrm{D}\right)$$

$$\frac{\partial \mathcal{G}\rho\theta'}{\partial t} + \nabla \cdot (\mathbf{v}\mathcal{G}\rho\theta') = \mathcal{G}\rho\left(-\widetilde{\mathbf{G}}^T\mathbf{u}\cdot\nabla\theta_a - \frac{L}{c_p\pi}\left(\frac{\Delta q_{vs}}{\Delta t} + E_r\right) + \mathcal{H}\right)$$

$$\frac{\partial \mathcal{G}\rho q_k}{\partial t} + \nabla \cdot (\mathbf{v}\mathcal{G}\rho q_k) = \mathcal{G}\rho\mathcal{R}^{q_k}$$

$$\frac{\partial \mathcal{G}\rho\varphi'}{\partial t} + \nabla \cdot (\mathbf{v}\mathcal{G}\rho\varphi') = \mathcal{G}\rho\sum_{\ell=1}^{3}\left(\frac{a_\ell}{\zeta_\ell}\nabla\cdot\zeta_\ell(\check{\mathbf{v}} - \widetilde{\mathbf{G}}^T\mathrm{C}\nabla\varphi')\right) + b\varphi' + c$$

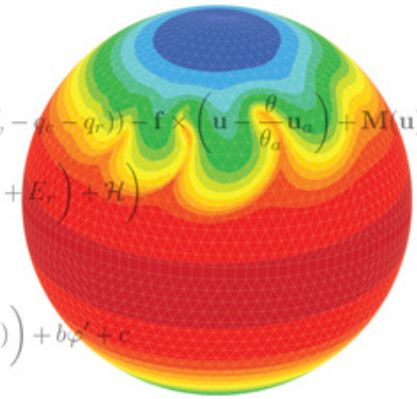

ECMWF

Operational configuration of the Integrated Forecasting System at ECMWF

Schematic of spectral-transform method in IFS

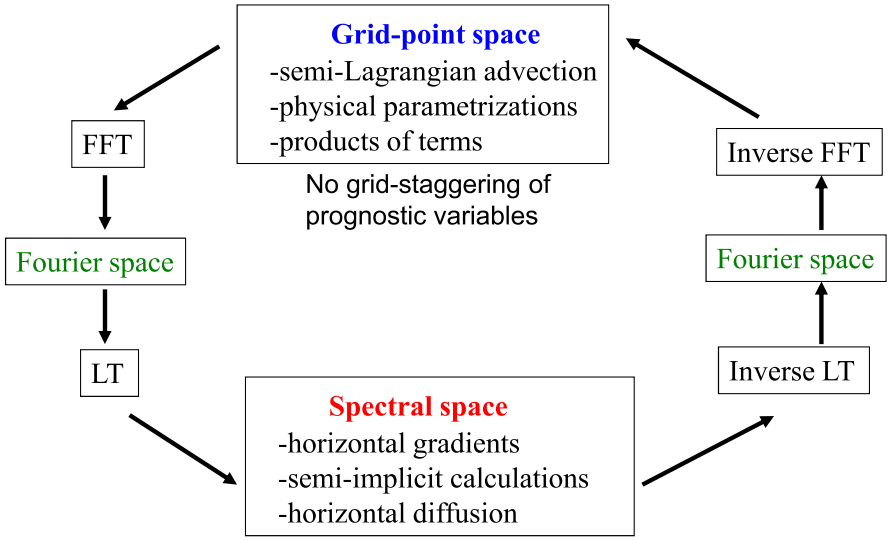

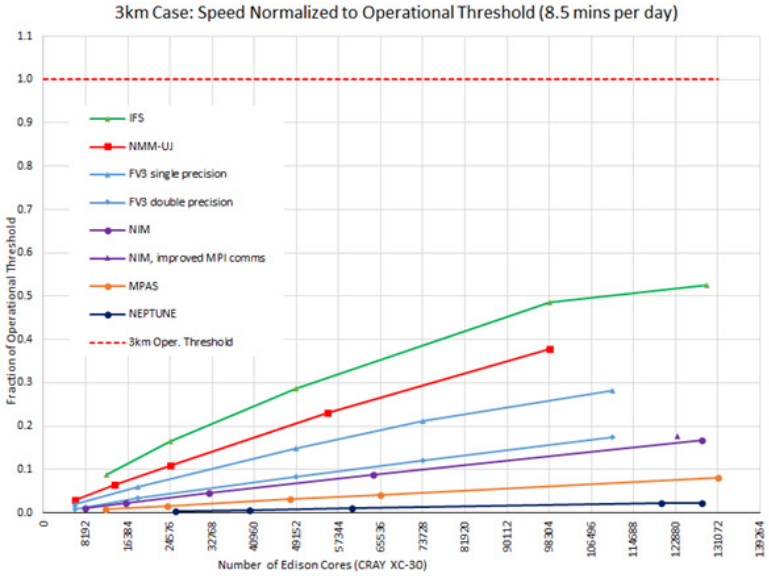

Current operational configuration of the Integrated Forecasting System (IFS) at the European Centre for Medium-Range Weather Forecasting:

- hydrostatic primitive equations (nonhydrostatic option available; see Benard et al. 2014)
- hybrid $\eta - p$ vertical coordinate (Simmons and Burridge, 1982)
- spherical harmonics representation in horizontal (Wedi et al., 2013)
- finite-element discretisation in vertical (Untch and Hortal, 2004)
- semi-implicit semi-Lagrangian (SISL) integration scheme (Temperton et al. 2001, Diamantakis 2014)
- cubic-octahedral ("TCo") grid (Wedi, 2014, Malardel et al. 2016)
- HRES: TCo1279 (O1280) with $\Delta_h \sim 9$ km and 137 vertical levels
- ENS (1+50 perturbed members): TCo639 (O640) with $\Delta_h \sim 16$ km and 91 vertical levels

Finite-Volume Module of the Integrated Forecasting System

⇒ ERC-funded project PantaRhei at ECMWF: prepare mathematical-numerical technology for future cloud-resolving Earth-system models

Enhance/complement IFS with a Finite-Volume Module (FVM) that introduces, among others:

→ numerics operating on compact stencils

→ local and global conservation

→ all-scale nonhydrostatic governing equations

→ flexible horizontal and vertical meshes

→ robustness and accuracy with regard to steep orography

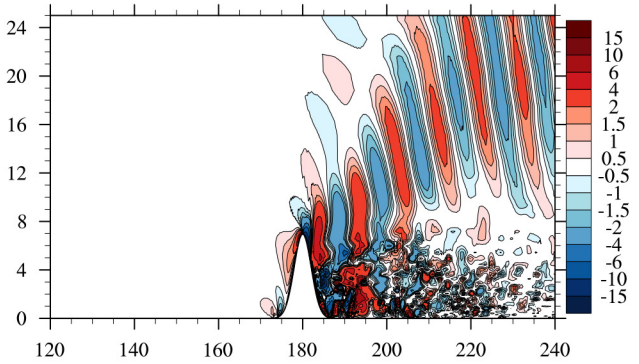

ECMWF

FVM formulation – key features

- deep-atmosphere nonhydrostatic Euler equations in geospherical framework (Szmelter and Smolarkiewicz 2010; Smolarkiewicz et al. 2016; Smolarkiewicz, Kühnlein, Grabowski 2017; Kühnlein, Malardel, Smolarkiewicz *in prep.*)
- flexible height-based terrain-following vertical coordinate
- hybrid of horizontally-unstructured median-dual finite-volume with vertically-structured finite-difference/finite-volume discretisation (Szmelter and Smolarkiewicz 2010; Smolarkiewicz et al. 2016)
- all prognostic variables are co-located
- two-time-level semi-implicit integration scheme with 3D implicit acoustic, buoyant and rotational modes (Smolarkiewicz, Kühnlein, Wedi JCP 2014)
- preconditioned generalised conjugate residual iterative solver for 3D elliptic problems arising in the semi-implicit integration schemes (Smolarkiewicz and Szmelter 2011 for a more recent review)
- non-oscillatory finite-volume MPDATA scheme (Smolarkiewicz and Szmelter 2005; Kühnlein and Smolarkiewicz 2017; Kühnlein, Klein, Smolarkiewicz *in prep.*)
- octahedral reduced Gaussian grid, but the FVM formulation not restricted to this (Szmelter and Smolarkiewicz 2016, see also Deconinck et al. 2017)
- optional moving mesh capability (as in Kühnlein, Smolarkiewicz, Dörnbrack 2012)

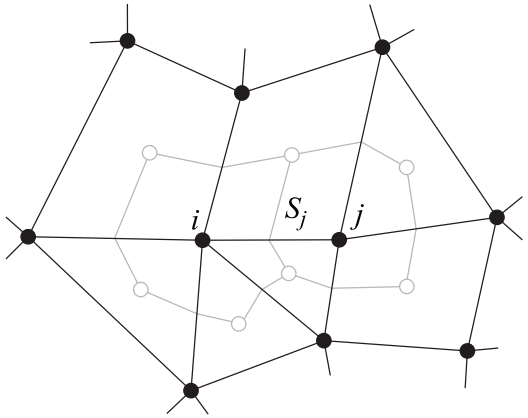

median-dual finite-volume approach

$$\int_\Omega \nabla\cdot\mathbf{A} = \int_{\partial\Omega} \mathbf{A}\cdot\mathbf{n} = \frac{1}{\mathcal{V}_i}\sum_{j=1}^{I(i)} A_j^{\perp} S_j$$

dual volume: $\mathcal{V}_i$, face area: S_j

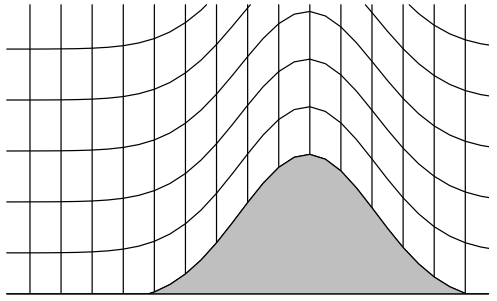

terrain-following coordinate

Octahedral reduced Gaussian grid

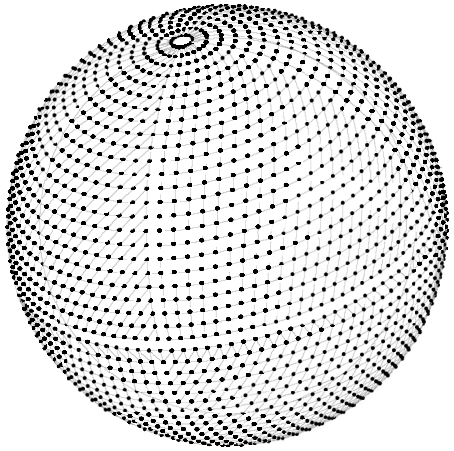

Nodes of octahedral grid 'O24'

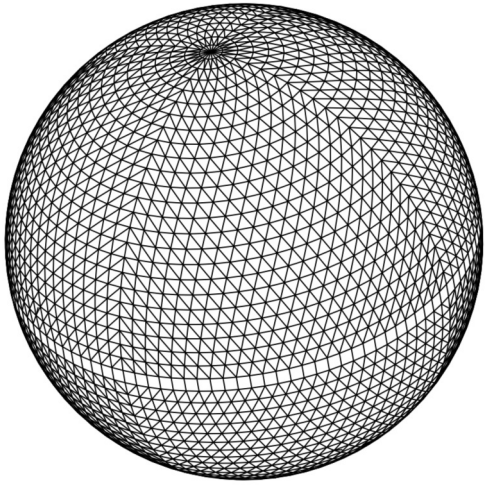

Primary mesh about nodes of octahedral grid in FVM

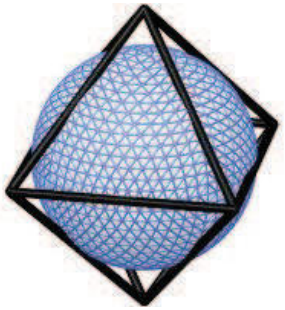

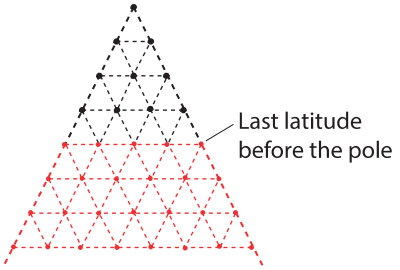

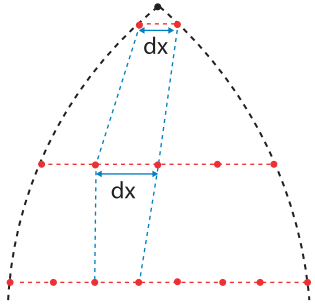

- octahedral reduced Gaussian grid (*octahedral grid* of size OX)
- suitable for spherical harmonics transforms applied in spectral IFS
  - → Gaussian latitudes ⇒ Legendre transforms
  - → equidistant distribution of nodes along latitudes following octahedral rule ⇒ Fourier transforms
- FVM develops median-dual mesh around nodes of octahedral grid

⇒ finite-volume and spectral-transform IFS can operate on same quasi-uniform horizontal grid

→ Malardel et al. ECMWF Newsletter 2016, Smolarkiewicz et al. JCP 2016

→ operational at ECMWF with HRES and ENS since March 2016

- Mesh generator and parallel data structures for FVM provided by ECMWF's Atlas framework (Deconinck et al. 2017)

Governing equations in FVM

Flux-form moist compressible Euler equations in generalised curvilinear coordinates (Smolarkiewicz, Kühnlein, Grabowski 2017; Kühnlein, Malardel, Smolarkiewicz *in prep.*):

$$\frac{\partial \mathcal{G}\rho}{\partial t} + \nabla \cdot (\mathbf{v}\mathcal{G}\rho) = 0$$

$$\frac{\partial \mathcal{G}\rho\mathbf{u}}{\partial t} + \nabla \cdot (\mathbf{v}\mathcal{G}\rho\mathbf{u}) = \rho\mathcal{G}\left(-\Theta_\rho \widetilde{\mathbf{G}}\nabla\varphi' + \mathbf{g}\mathcal{B} - \mathbf{f}\times\left(\mathbf{u} - \frac{\theta_\rho}{\theta_{\rho a}}\mathbf{u}_a\right) + \mathbf{M}(\mathbf{u}) + \mathbf{D}\right)$$

$$\frac{\partial \rho\mathcal{G}\theta'}{\partial t} + \nabla \cdot \left(\mathbf{v}\rho\mathcal{G}\,\theta'\right) = \rho\mathcal{G}\left(-\widetilde{\mathbf{G}}^T\mathbf{u}\cdot\nabla\theta_a + \mathcal{H}\right)$$

$$\varphi' = c_p\theta_0\left[\left(\frac{R_d}{p_0}\rho\theta(1+q_v/\epsilon)\right)^{R_d/c_v} - \pi_a\right]$$

$$\frac{\partial \rho\mathcal{G}q_k}{\partial t} + \nabla\cdot(\mathbf{v}\rho\mathcal{G}q_k) = \rho\mathcal{G}R^{q_k} \qquad \text{where} \quad q_k = q_v, q_c, q_r, q_i, q_s$$

with:

$$\mathbf{v} = \widetilde{\mathbf{G}}^T\mathbf{u}\ , \qquad \Theta_\rho := \frac{\theta\,(1+q_v/\epsilon)}{\theta_0\,(1+q_t)} \equiv \frac{\theta_\rho}{\theta_0}\ , \qquad \epsilon := \frac{R_d}{R_v}\ , \qquad \theta' := \theta - \theta_a\ ,$$

$$\mathcal{B} \equiv \left(1 - \frac{\theta_a}{\theta_{\rho a}}\eta_{\theta_\rho} - \frac{\theta'}{\theta_{\rho a}}\eta_{\theta_\rho}\right)\ , \qquad \eta_{\theta_\rho} \equiv \frac{1+q_v/\epsilon}{1+q_t}\ , \qquad q_t = \sum_k q_k$$

Finite-volume and spectral-transform solutions in IFS

Dry baroclinic instability with finite-volume (FV) and spectral-transform (ST) methods in IFS using O640/TCo639:

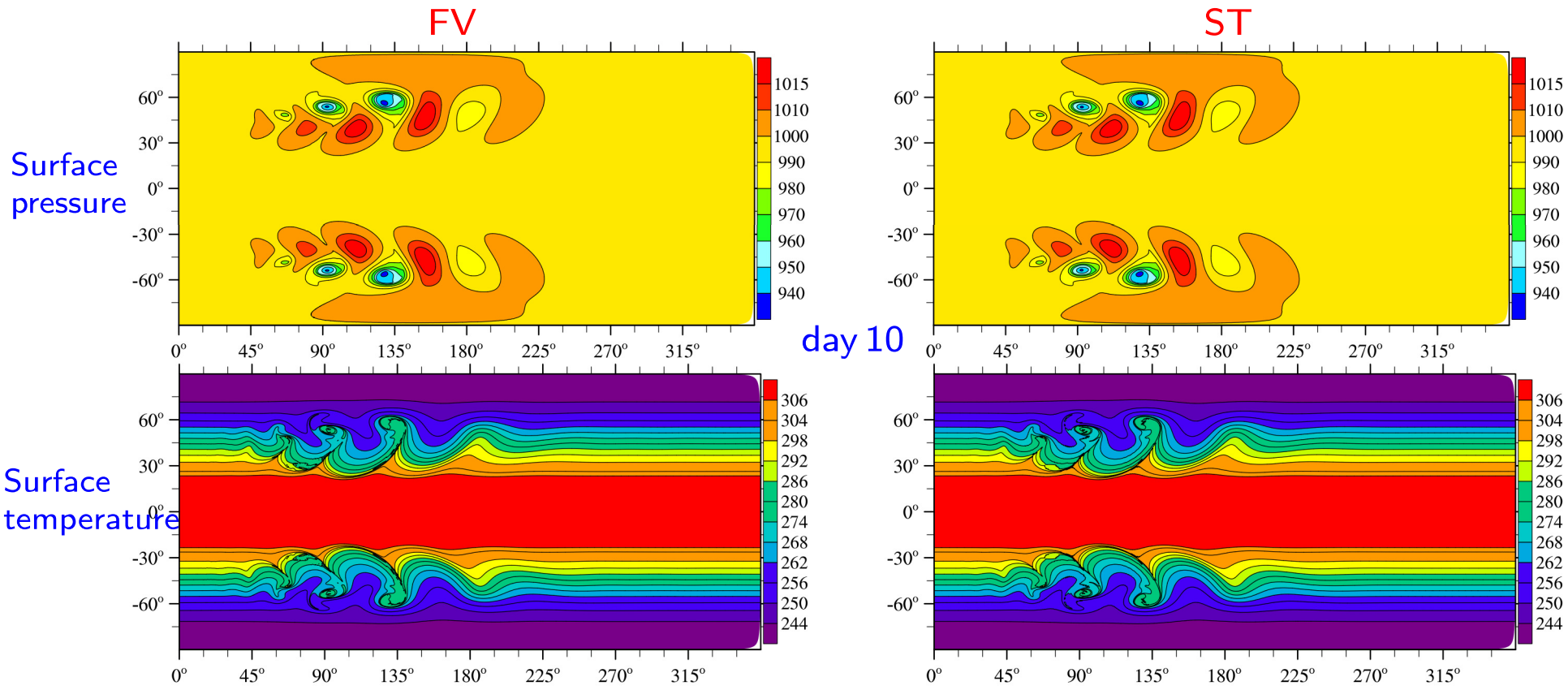

Setup of baroclinic instability according to Ullrich et al. QJ 2014 triggered by perturbation of u-velocity as in DCMIP

Finite-volume and spectral-transform solutions in IFS

Dry baroclinic instability with finite-volume (FV) and spectral-transform (ST) methods in IFS using O640/TCo639:

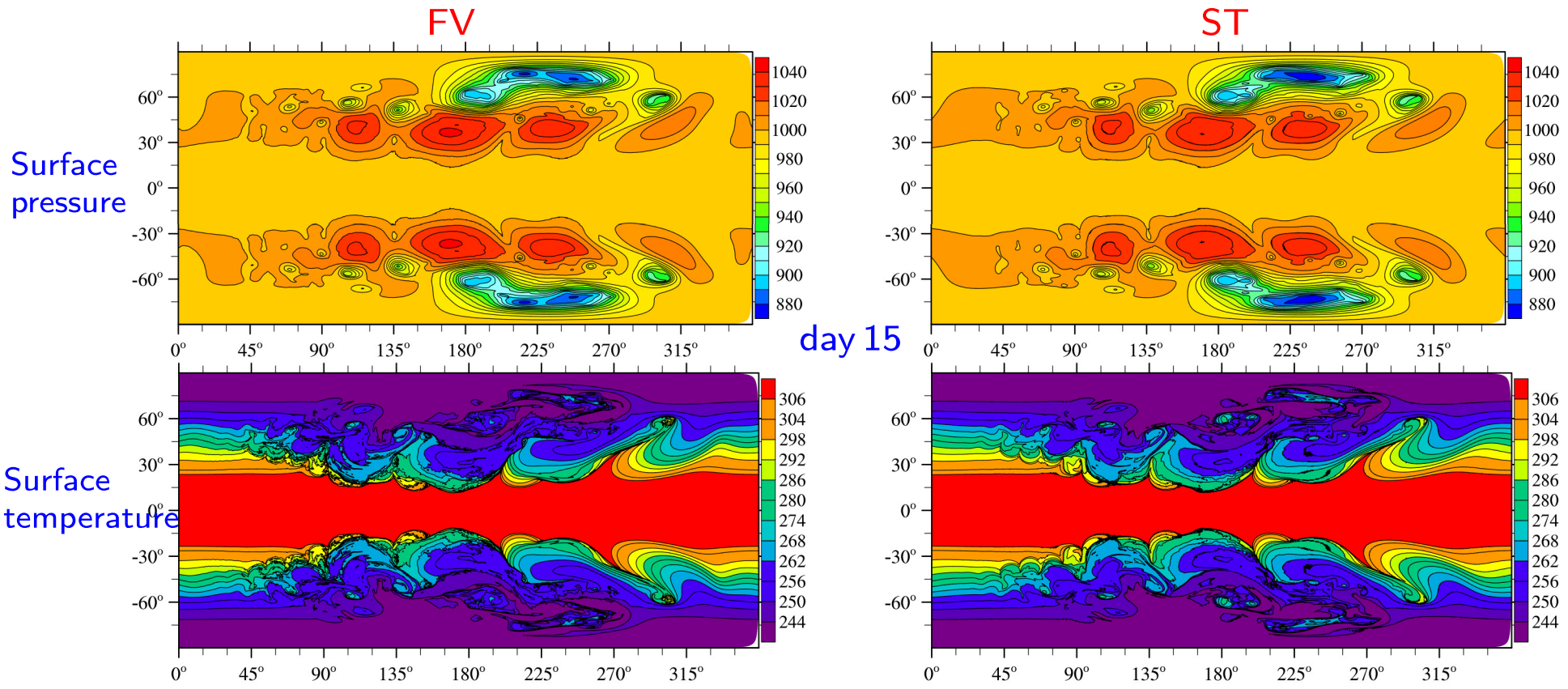

Finite-volume and spectral-transform solutions in IFS

Dry baroclinic instability with FV and ST at two different horizontal resolutions:

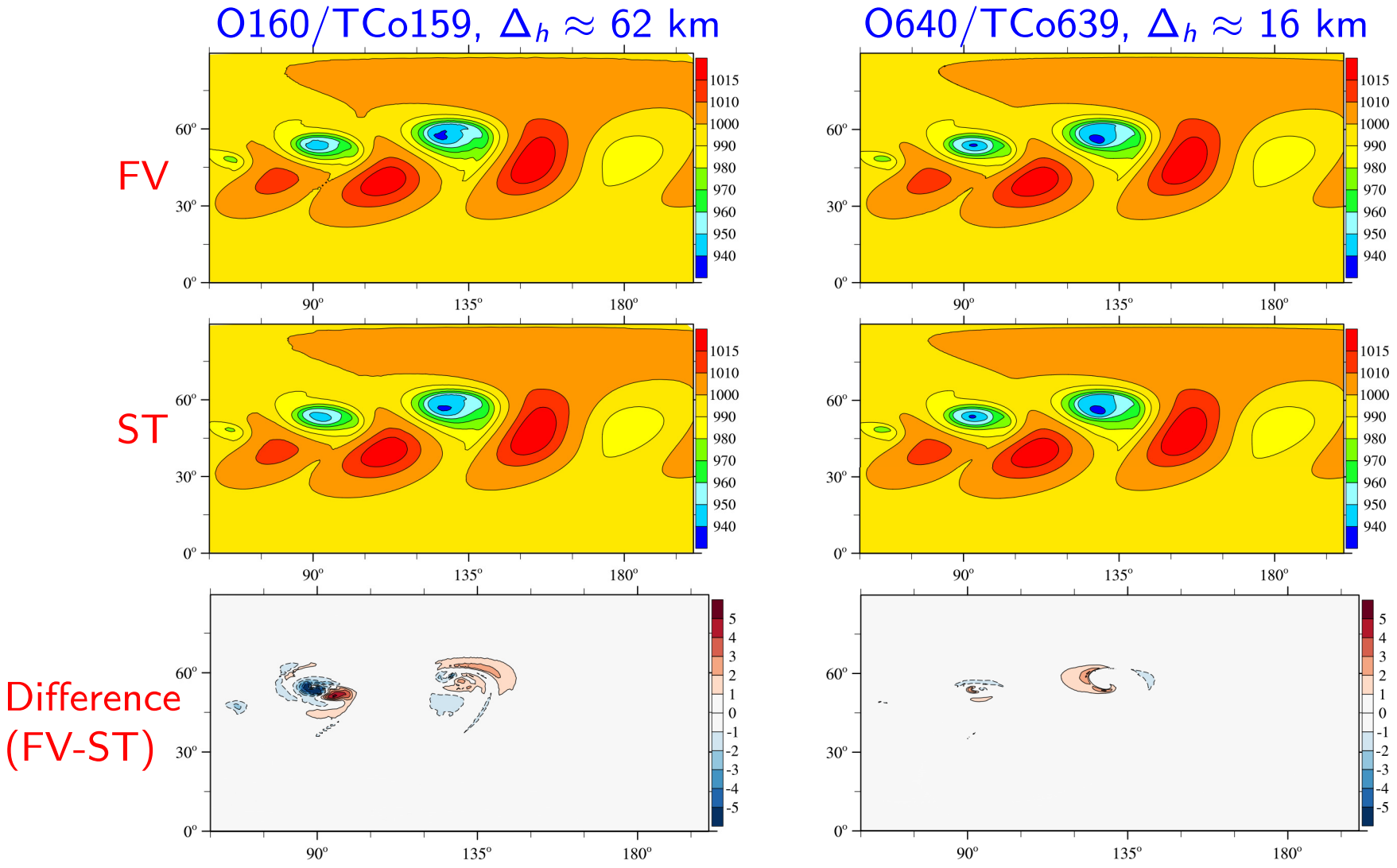

Surface pressure (hPa) at day 10

Finite-volume and spectral-transform solutions in IFS

Dry baroclinic instability with FV and ST methods using O640/TCo639:

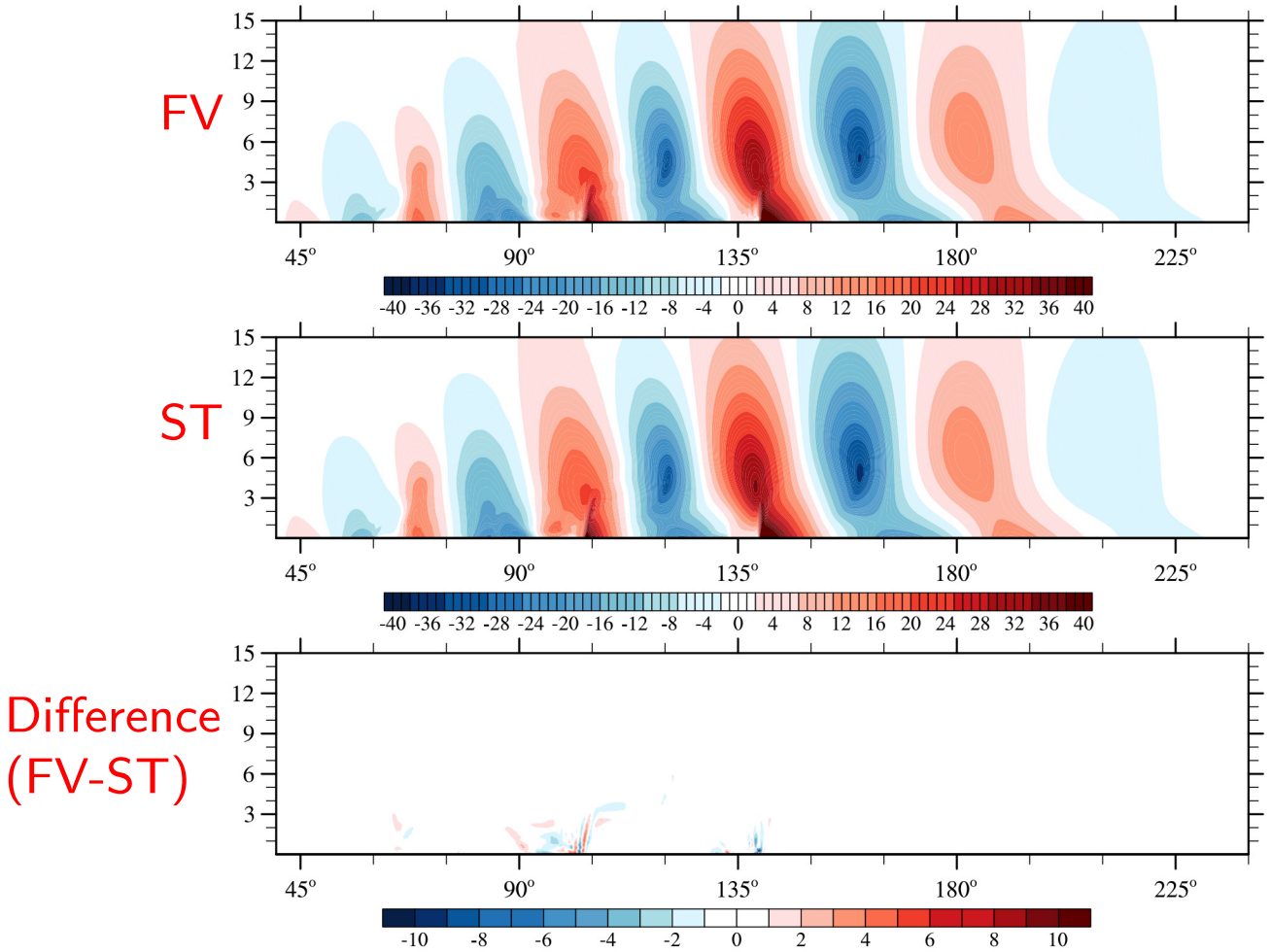

Meridional wind (m/s) in zonal-height section at 50° N, day 10

Finite-volume and spectral-transform solutions in IFS

Dry baroclinic instability with FV and ST methods using O640/TCo639:

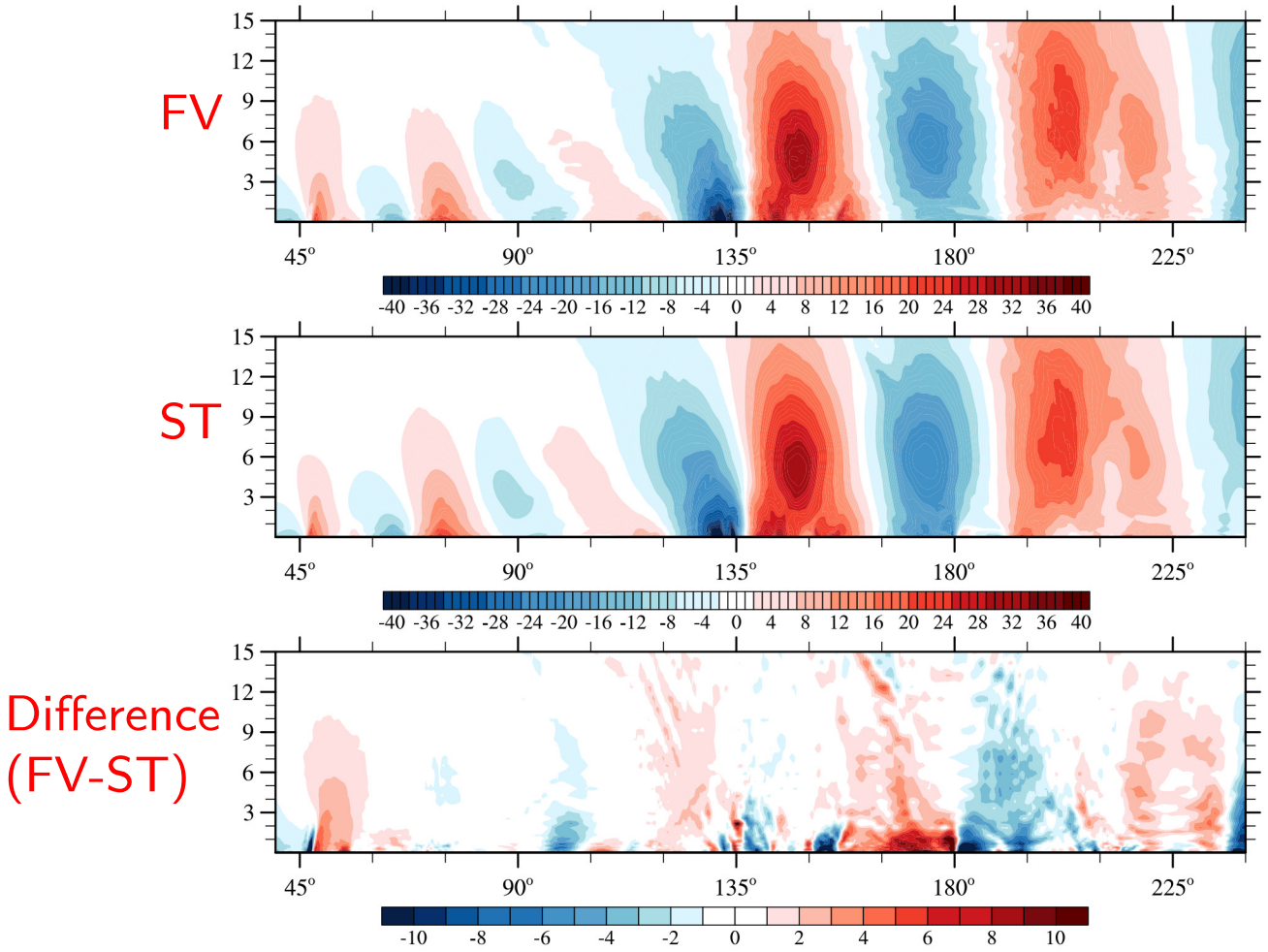

Meridional wind (m/s) in zonal-height section at 50° N, day 15

Finite-volume and spectral-transform solutions in IFS

Instantaneous kinetic energy spectra O640/TCo639 ($\Delta_h \approx 16$ km) for baroclinic instability at day 15

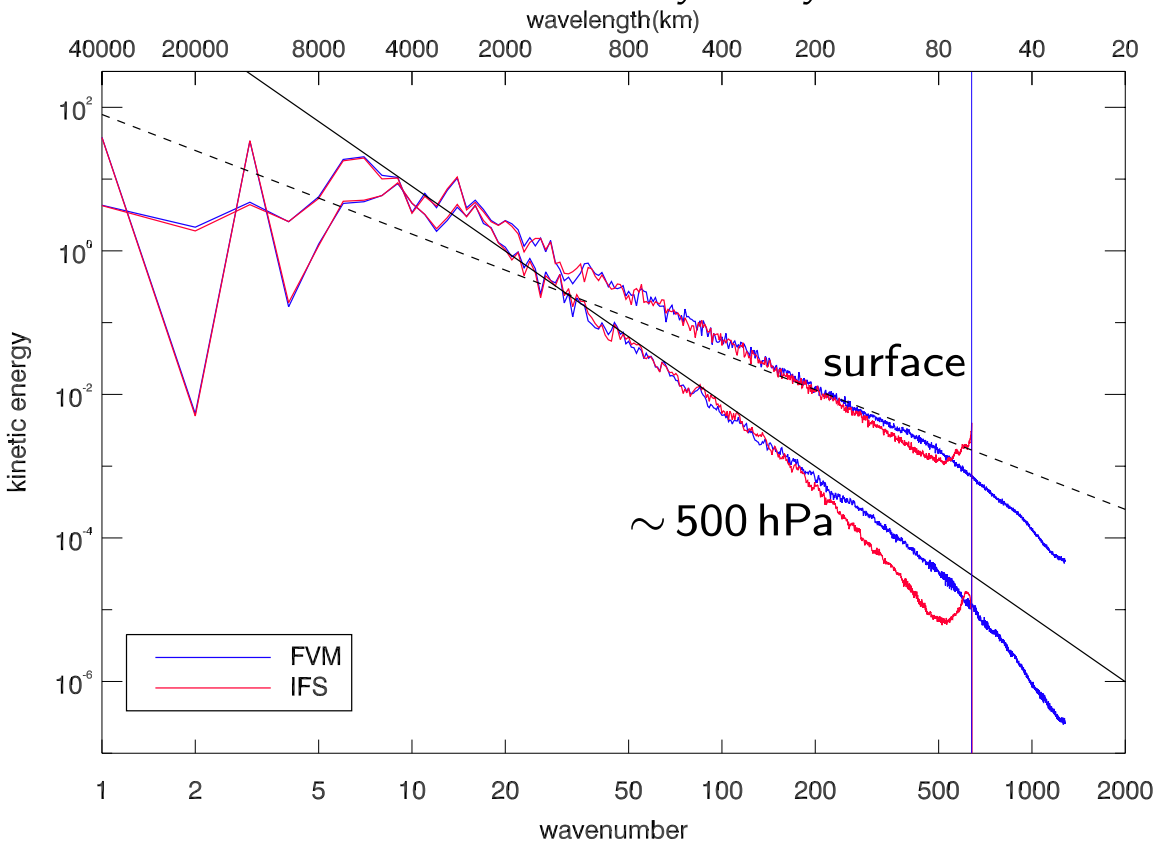

Finite-volume and spectral-transform solutions in IFS

Moist baroclinic instability with large-scale condensation and diagnostic rain (Reed and Jablonowski 2011):

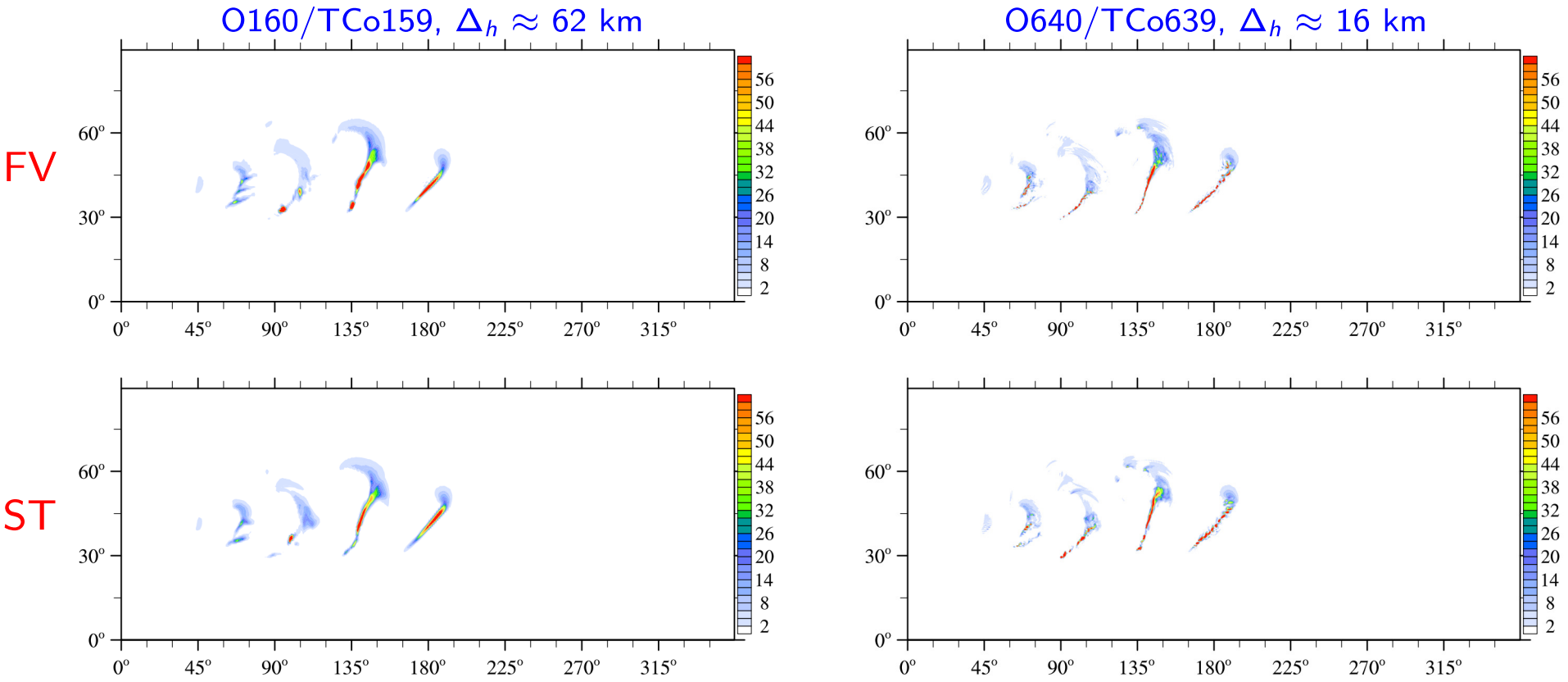

Diagnostic precipitation (mm/day) at day 10

Finite-volume and spectral-transform solutions in IFS

Moist baroclinic instability with large-scale condensation and diagnostic rain (Reed and Jablonowski 2011):

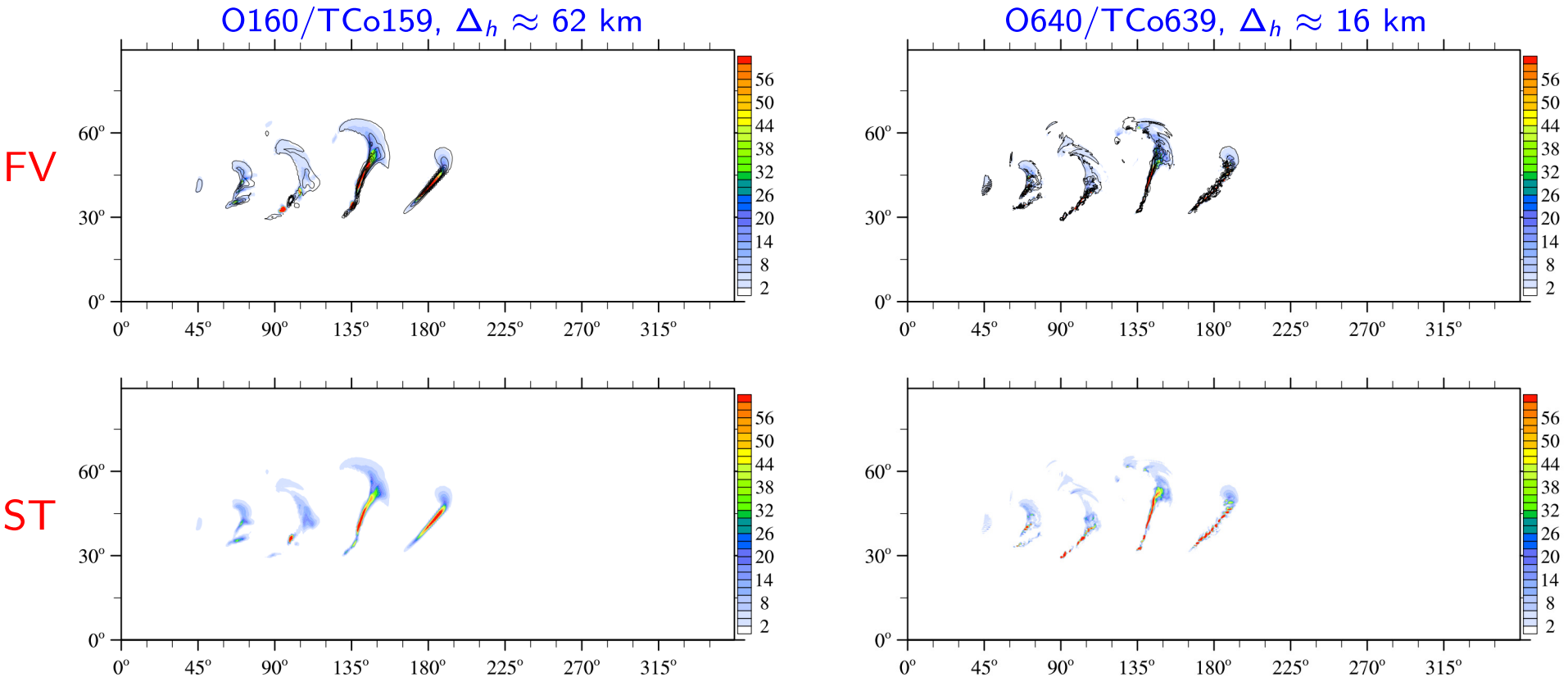

Diagnostic precipitation (mm/day) at day 10

Finite-volume and spectral-transform solutions in IFS

Moist baroclinic instability with large-scale condensation and diagnostic rain (Reed and Jablonowski 2011):

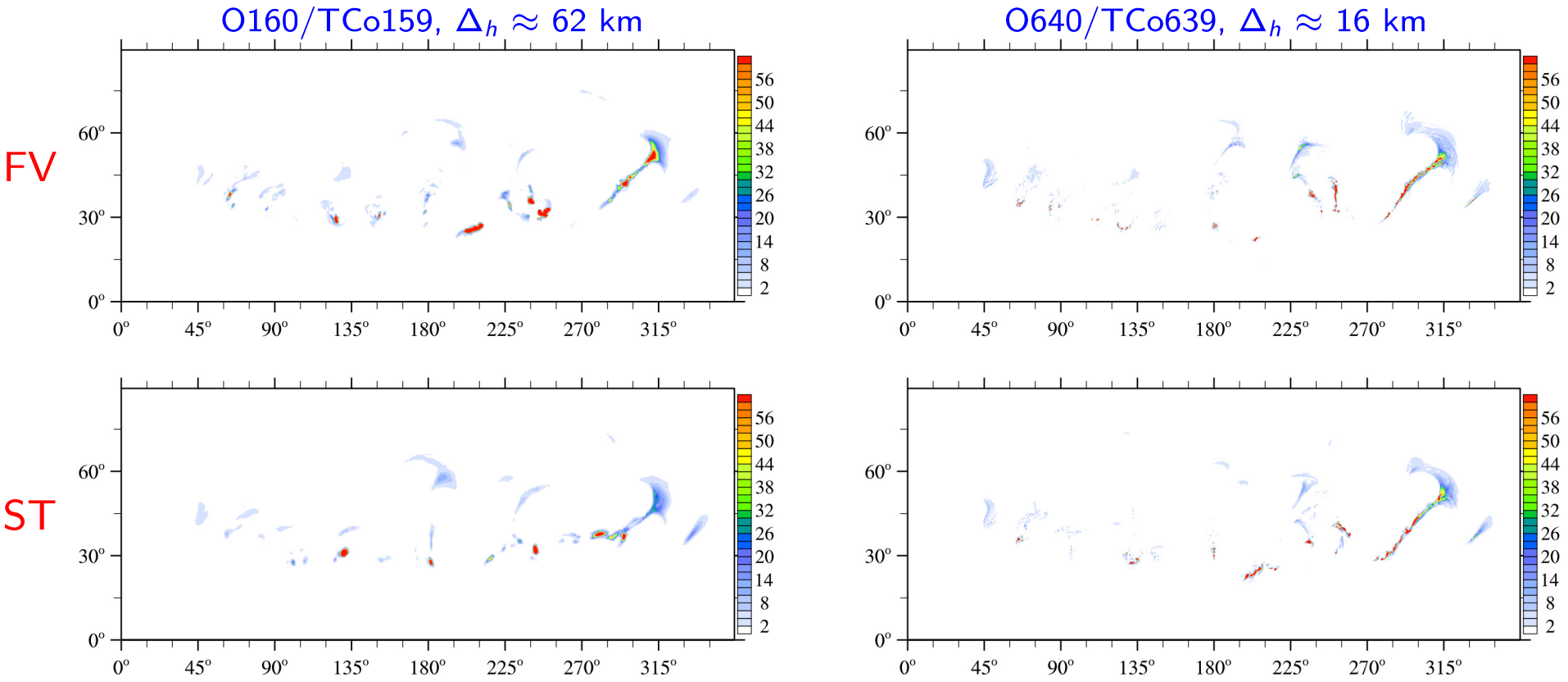

Diagnostic precipitation (mm/day) at day 15

Finite-volume and spectral-transform solutions in IFS

Moist baroclinic instability with large-scale condensation and diagnostic rain (Reed and Jablonowski 2011):

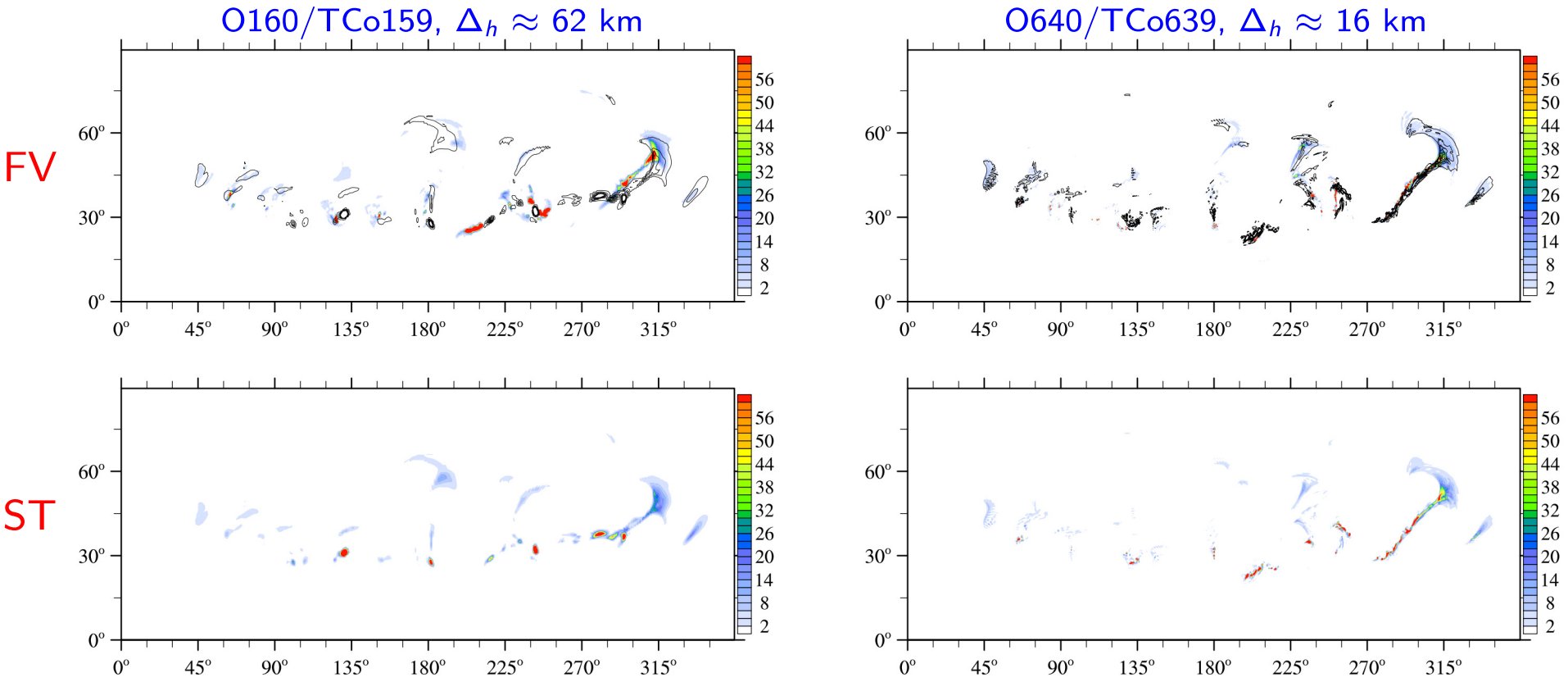

Diagnostic precipitation (mm/day) at day 15

Finite-volume and spectral-transform solutions in IFS

Moist baroclinic instability using simplified physical parametrisations (Reed and Jablonowski, 2012):

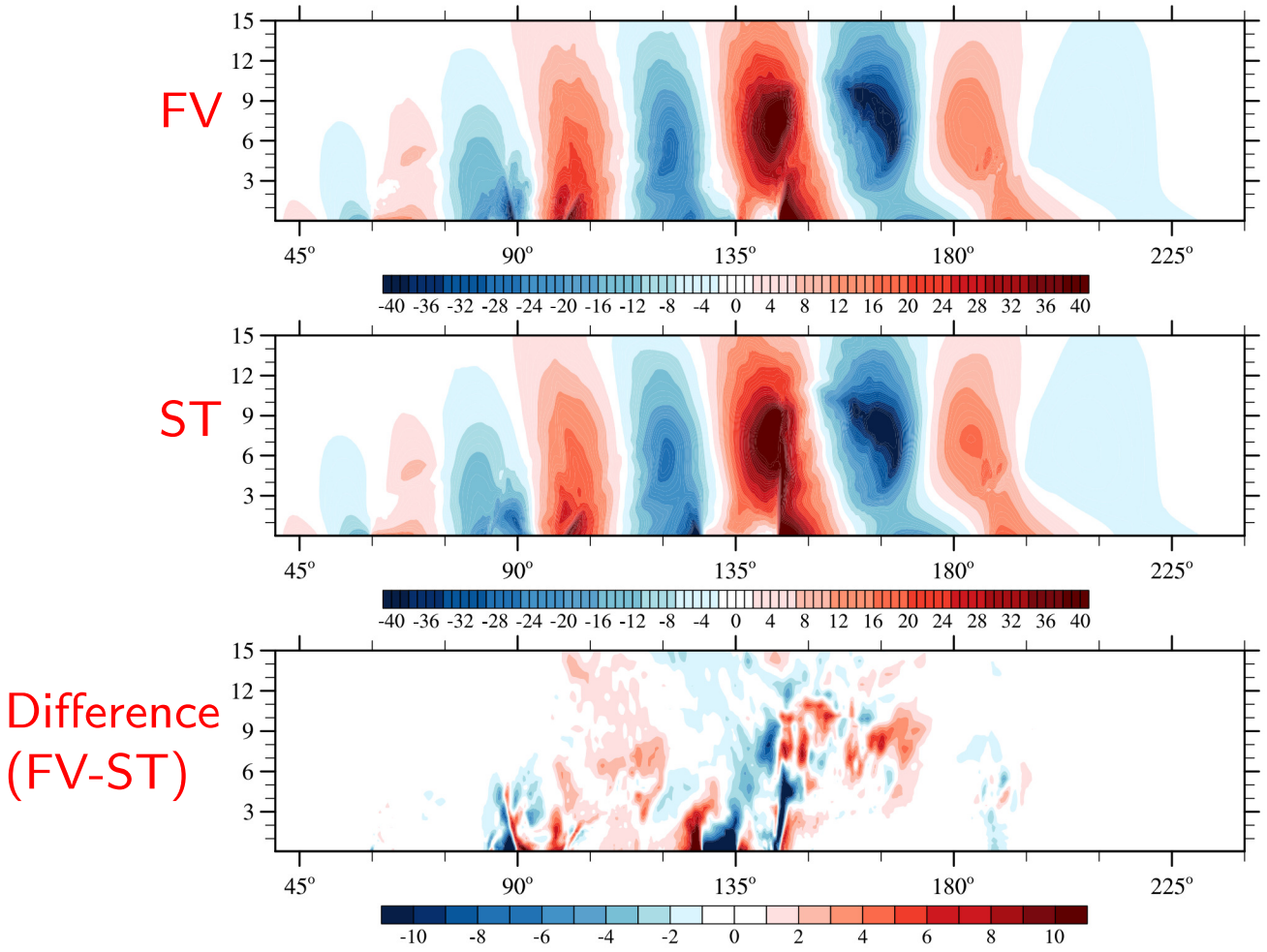

Meridional wind (m/s) in zonal-height section at 50° N, day 10

Finite-volume and spectral-transform solutions in the IFS

Moist baroclinic instability using simplified physical parametrisations (Reed and Jablonowski, 2012):

Instantaneous kinetic energy spectra O640/TCo639 ($\Delta_h \approx 16$ km) for moist baroclinic instability at day 15

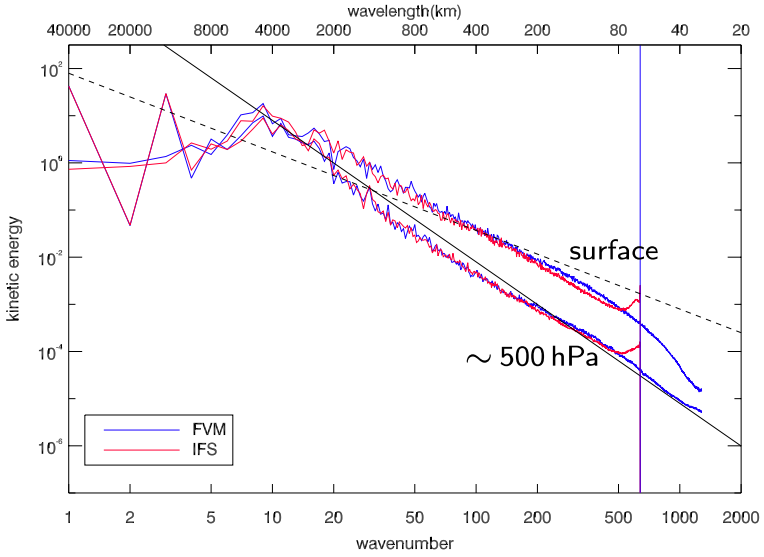

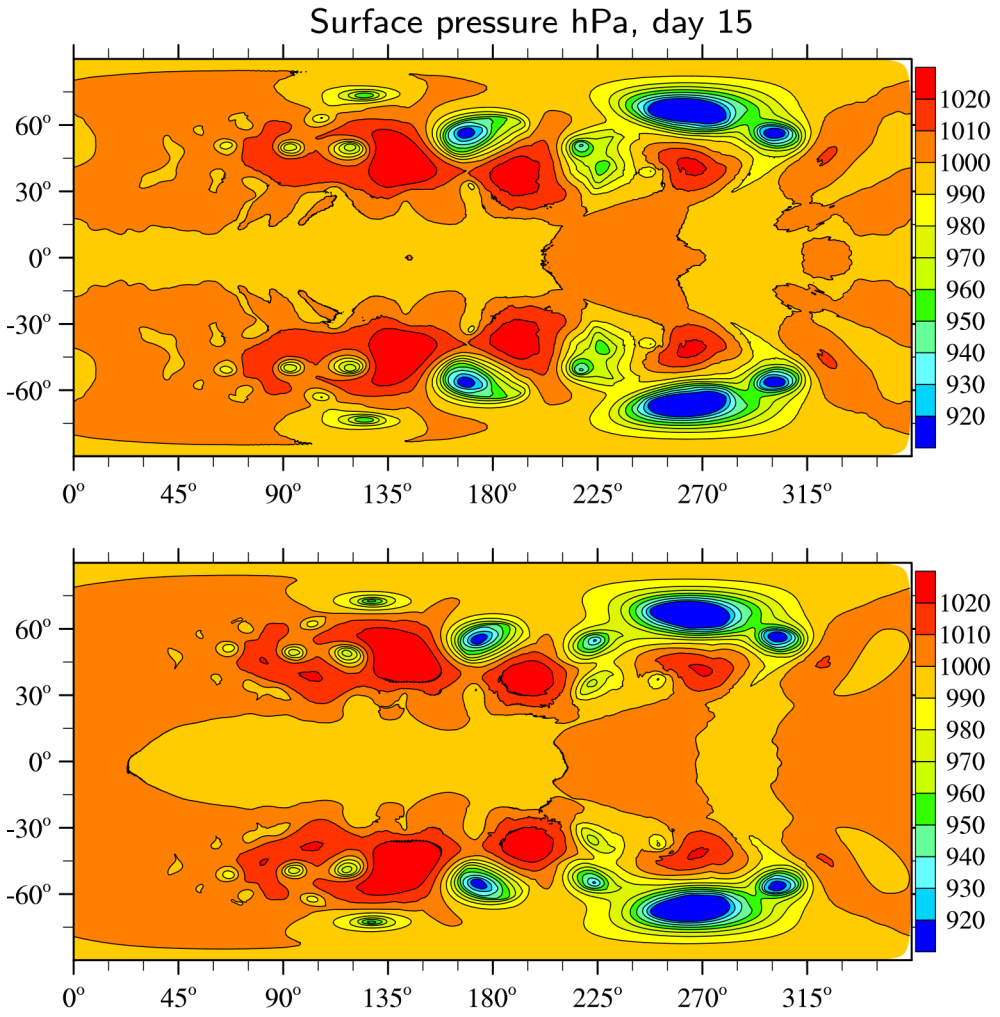

Tropical cyclone simulations

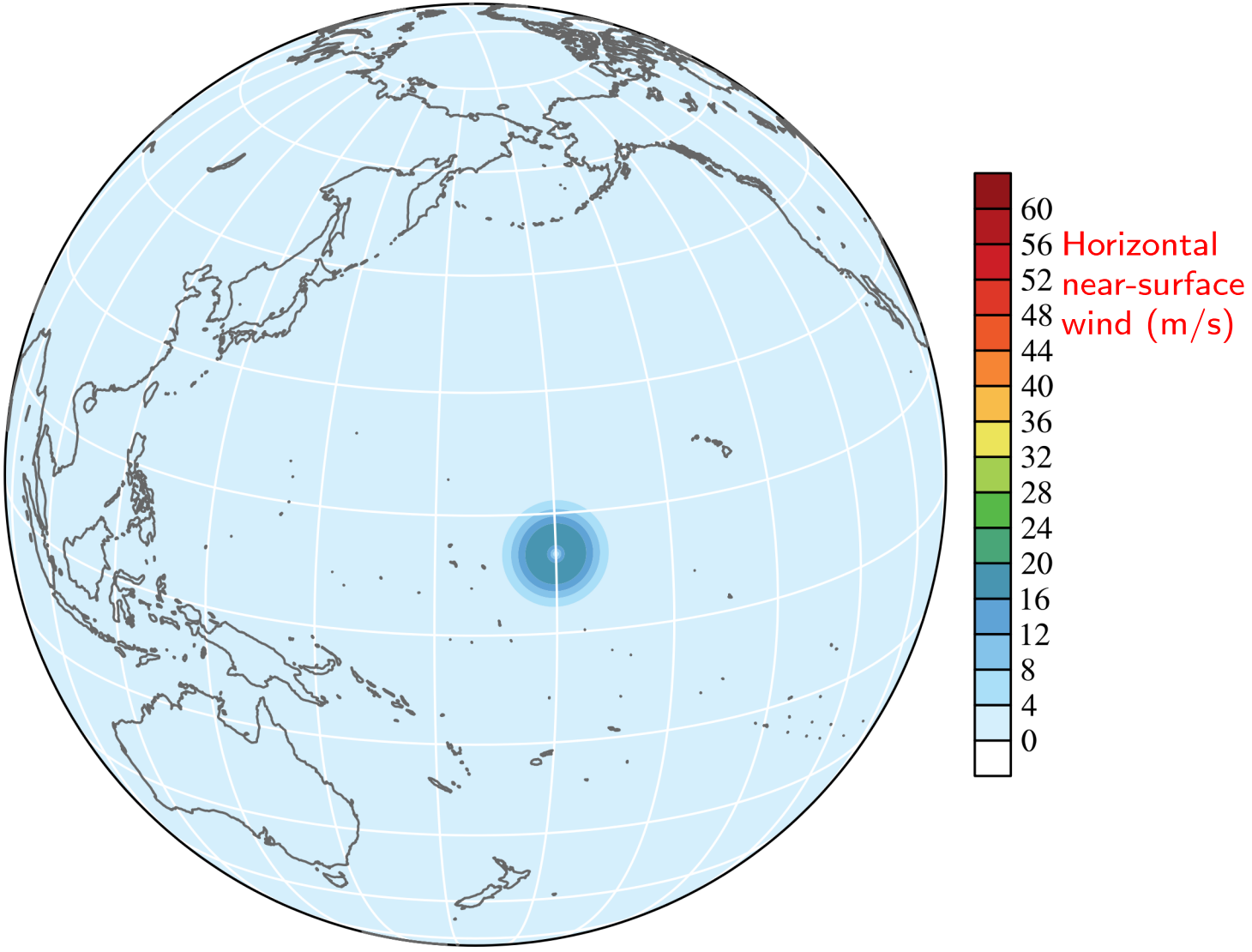

Tropical cyclone simulations (over 10 days) on aqua-planet with parametrisations for large-scale condensation with diagnostic rain, surface fluxes and PBL diffusion (Reed and Jablonowski 2011)

ECMWF

Tropical cyclone simulations

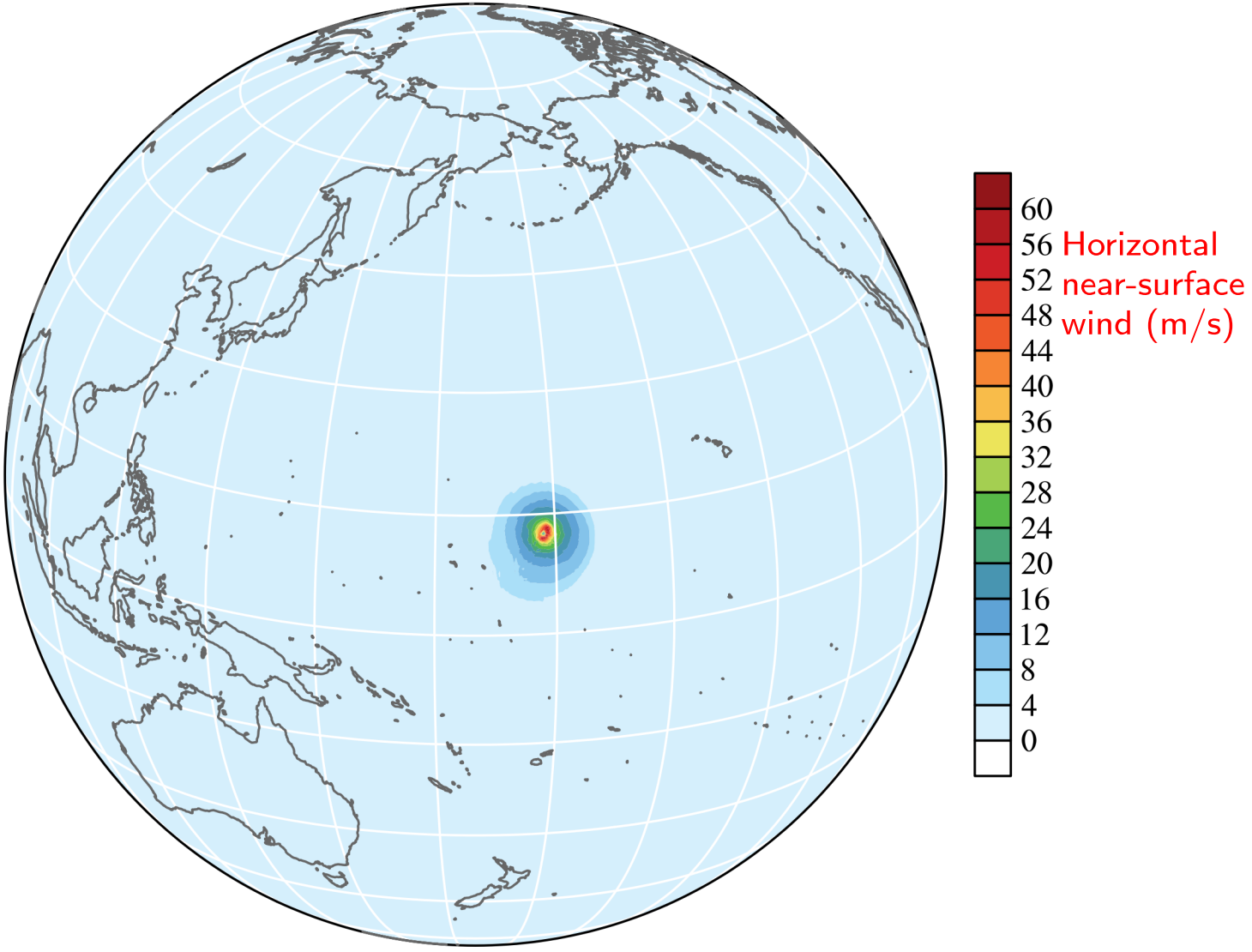

Tropical cyclone simulations (over 10 days) on aqua-planet with parametrisations for large-scale condensation with diagnostic rain, surface fluxes and PBL diffusion (Reed and Jablonowski 2011)

ECMWF

Tropical cyclone simulations

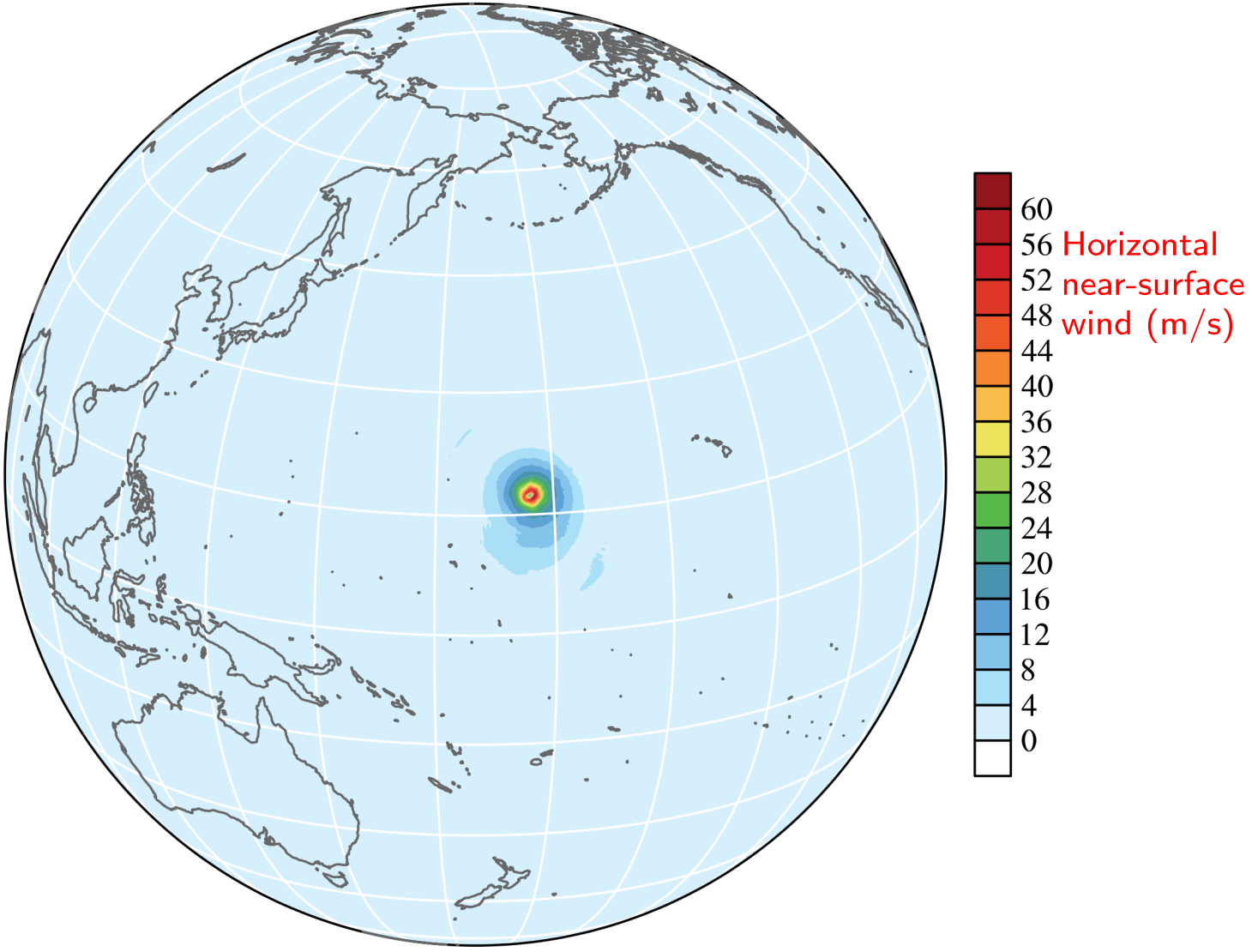

Tropical cyclone simulations (over 10 days) on aqua-planet with parametrisations for large-scale condensation with diagnostic rain, surface fluxes and PBL diffusion (Reed and Jablonowski 2011)

ECMWF

Tropical cyclone simulations

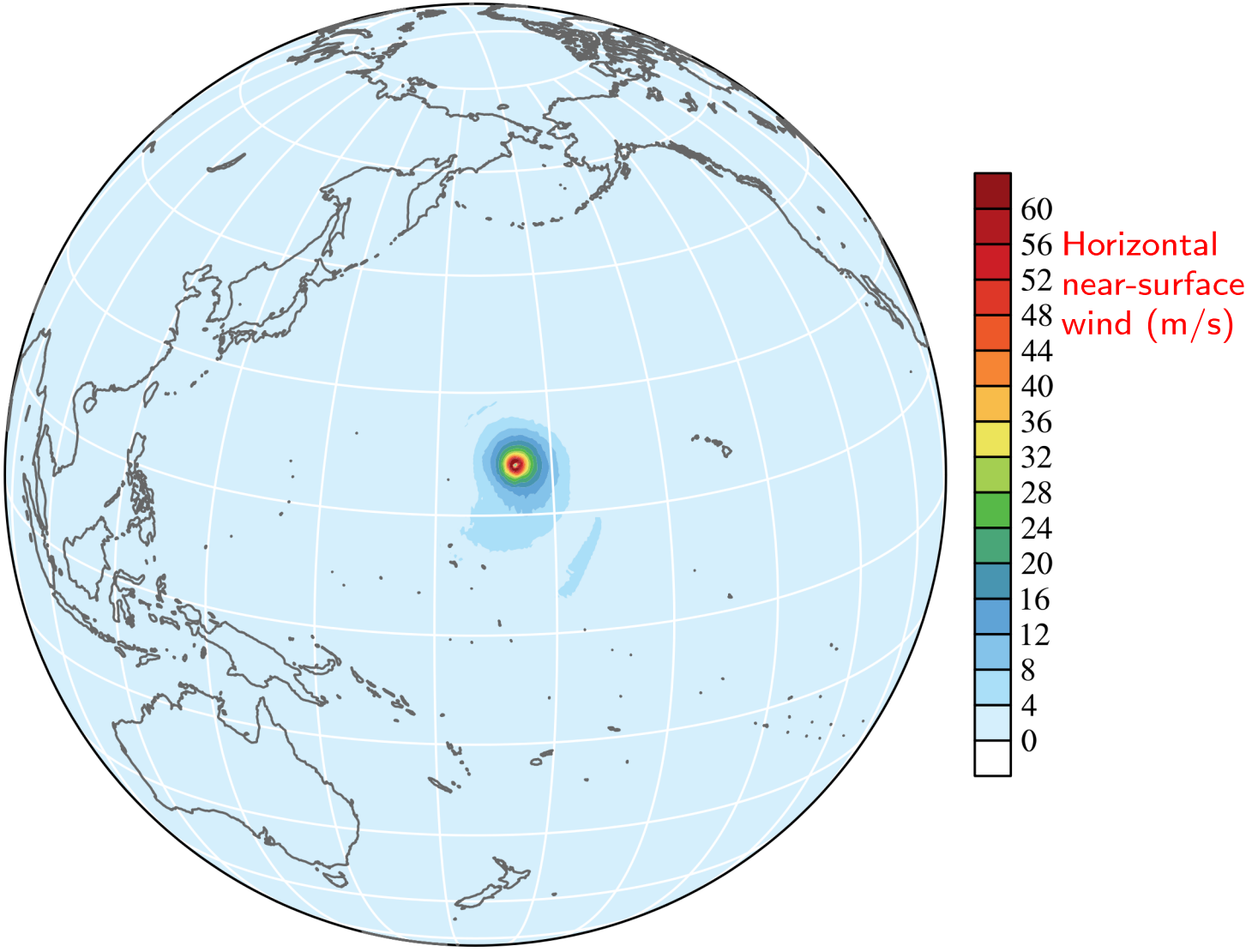

Tropical cyclone simulations (over 10 days) on aqua-planet with parametrisations for large-scale condensation with diagnostic rain, surface fluxes and PBL diffusion (Reed and Jablonowski 2011)

ECMWF

Tropical cyclone simulations

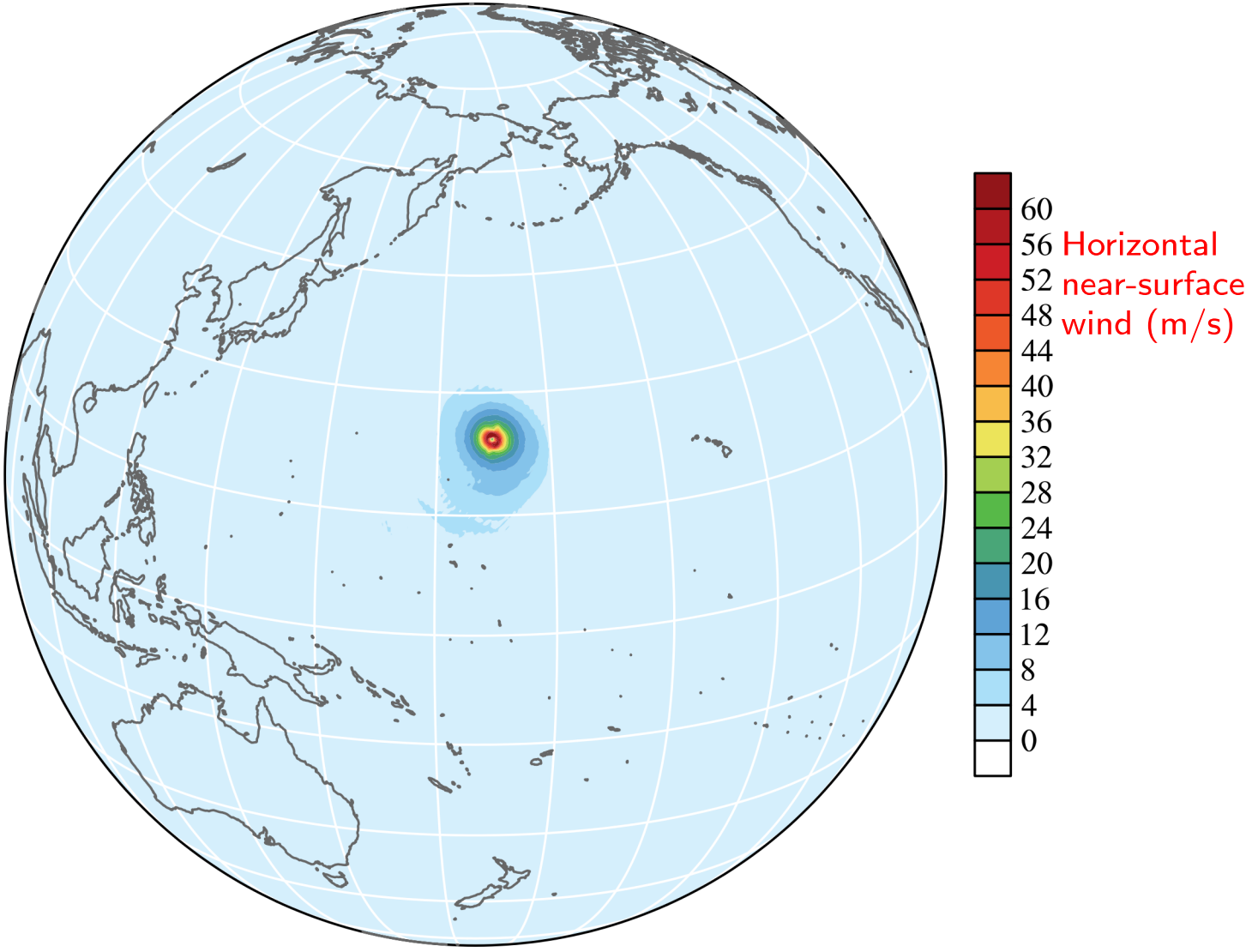

Tropical cyclone simulations (over 10 days) on aqua-planet with parametrisations for large-scale condensation with diagnostic rain, surface fluxes and PBL diffusion (Reed and Jablonowski 2011)

ECMWF

Tropical cyclone simulations

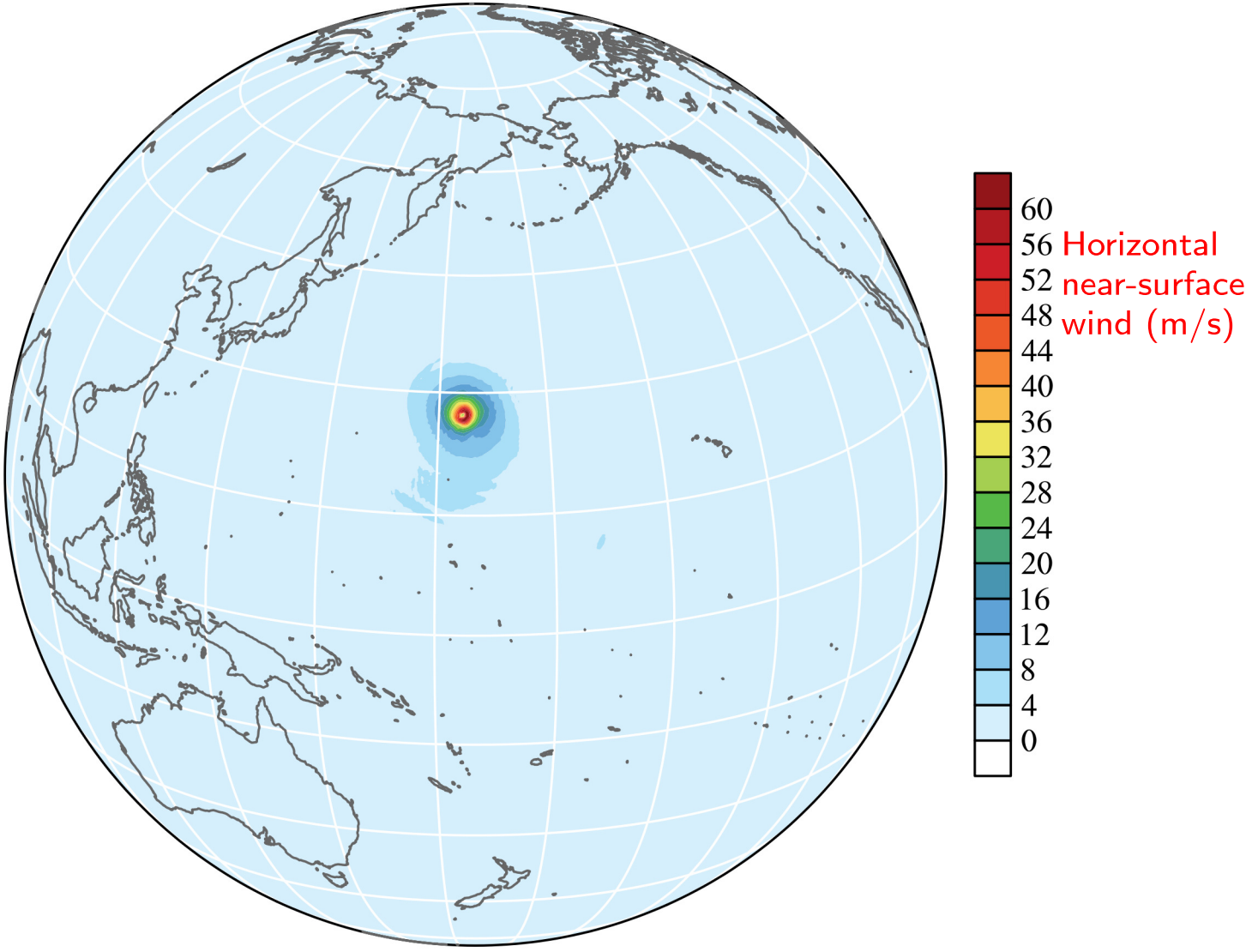

Tropical cyclone simulations (over 10 days) on aqua-planet with parametrisations for large-scale condensation with diagnostic rain, surface fluxes and PBL diffusion (Reed and Jablonowski 2011)

ECMWF

Tropical cyclone simulations with FV and ST approaches in IFS

Tropical cyclone simulations with coupling to parametrisations for large-scale condensation with diagnostic rain, surface fluxes and PBL diffusion (Reed and Jablonowski 2011) on O640/L60:

Wind speed (m/s) in horizontal section at $z \approx 1$ km:

Wind speed (m/s) in zonal-height section:

FV

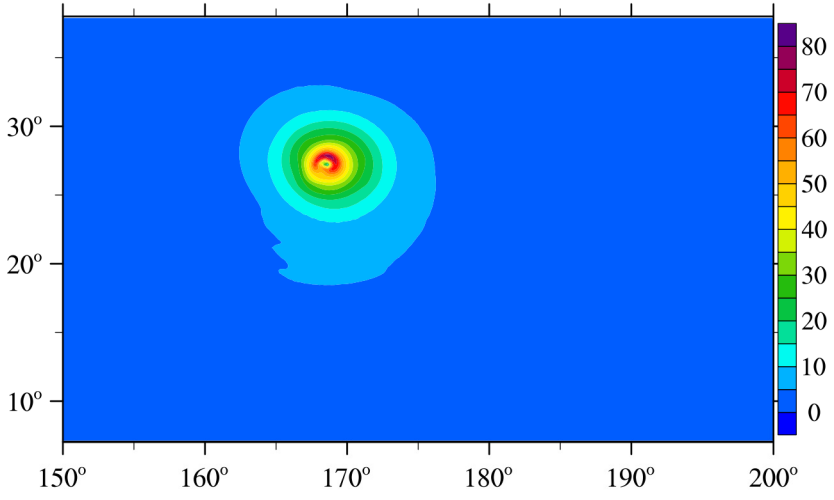

day 10

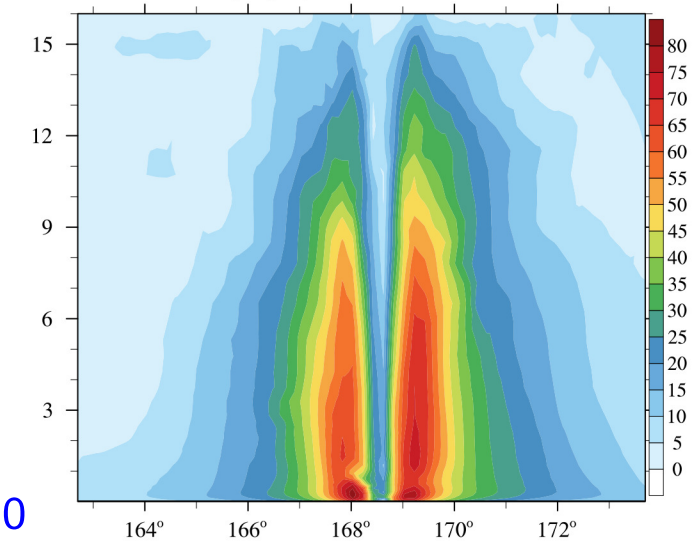

ST

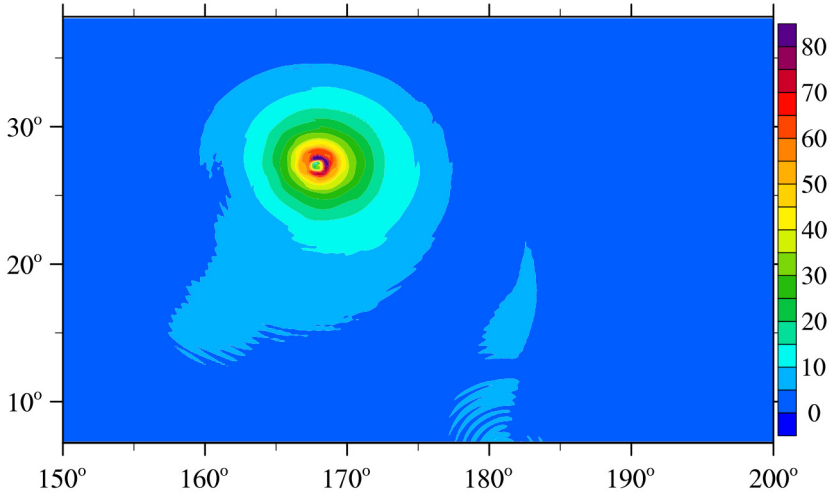

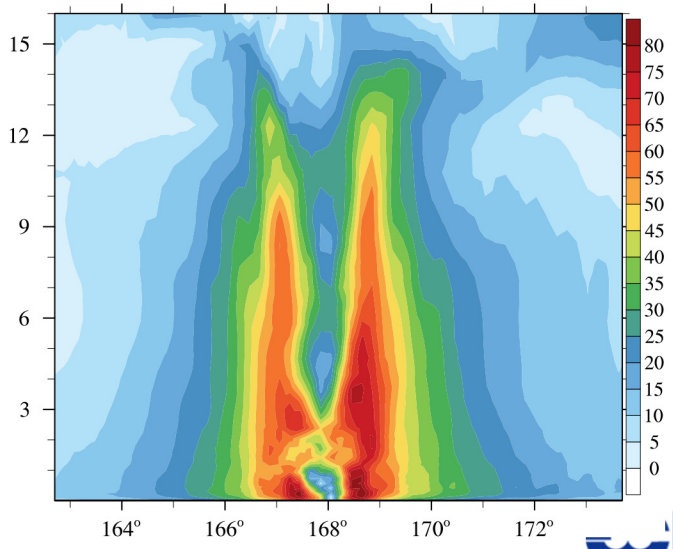

ECMWF

Orography in FVM

Held-Suarez climate benchmark O640 (16 km) with realistic IFS orography at day 90 (relative vorticity at z=2 km)

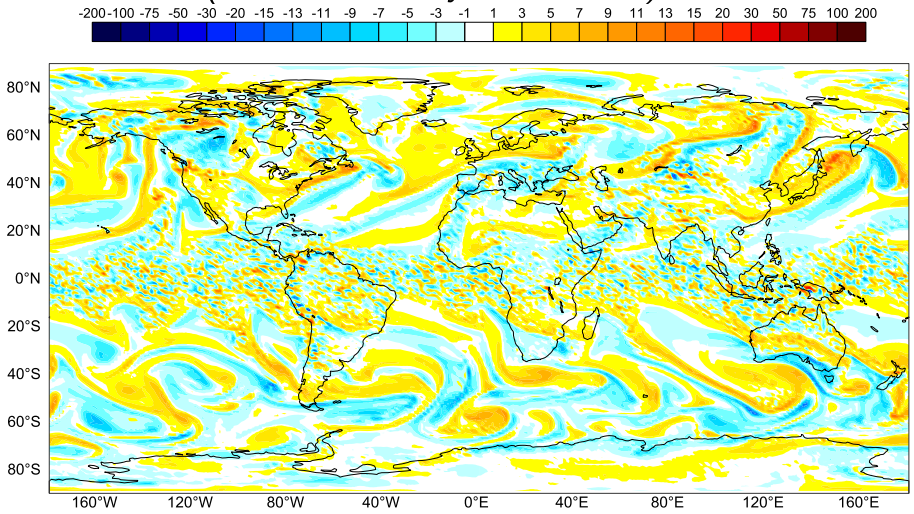

terrain-following coordinates

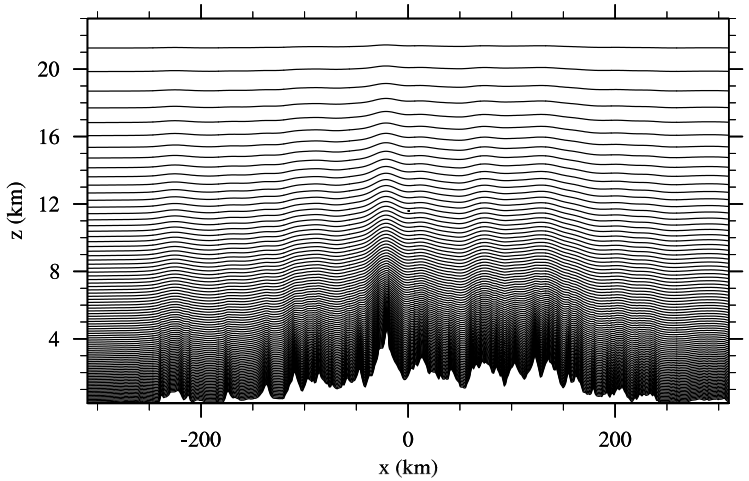

stratified flow past steep orography with maximum slope $\sim 70^\circ$ on a reduced-radius planet after 2 h (vertical velocity in m/s, lon-height section at lat=0, lon-lat section at z=2 km), cf. Zängl MWR 2012

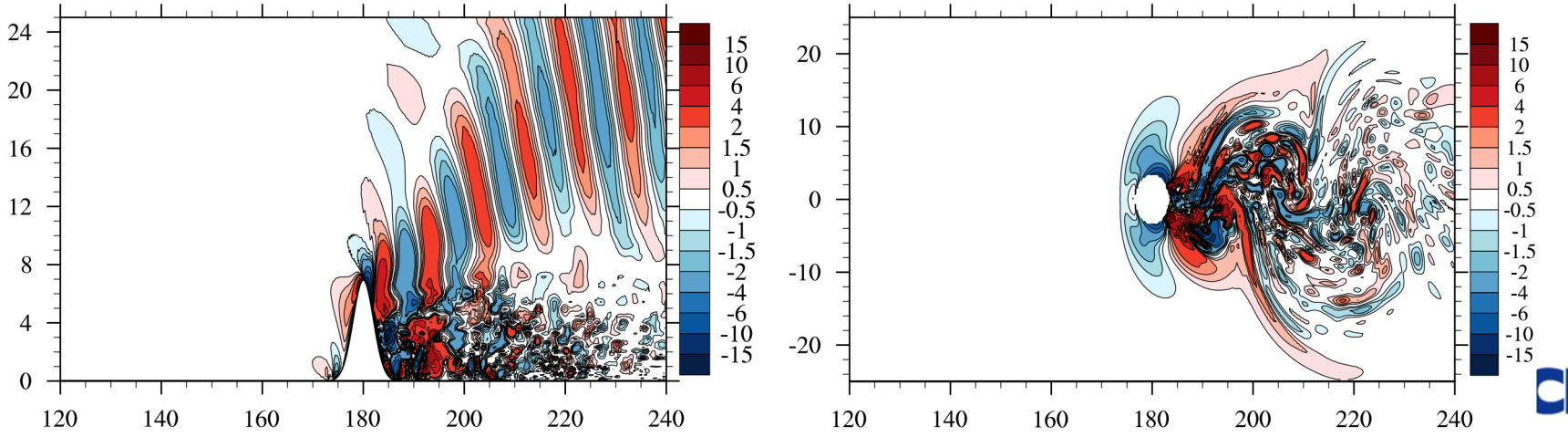

Dynamical Core Model Intercomparison Project (DCMIP)

Time evolution of supercells at 1km resolution

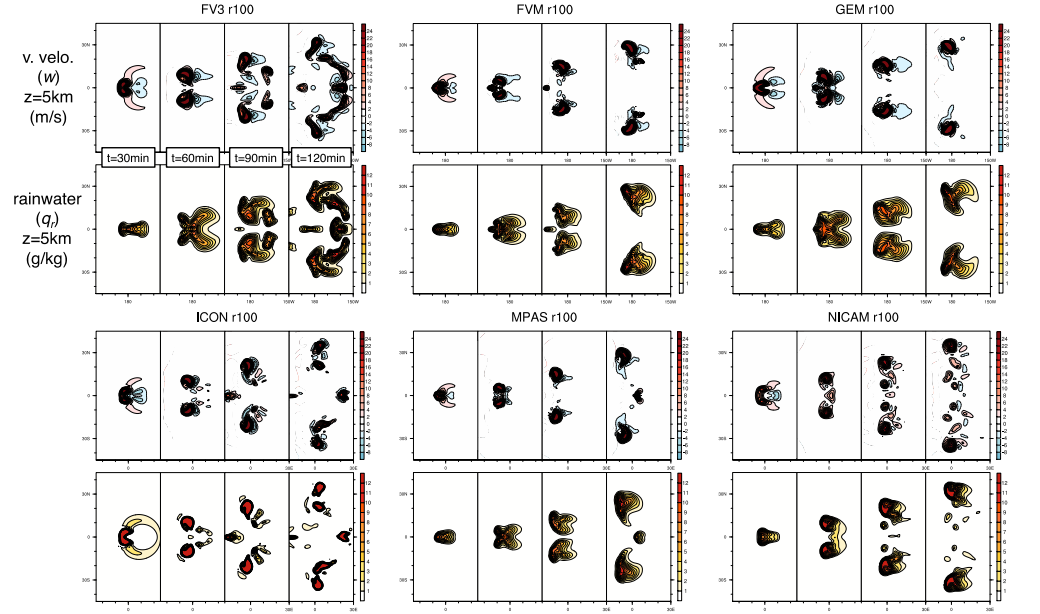

Geosci. Model Dev. Discuss., https://doi.org/10.5194/gmd-2017-108
Manuscript under review for journal Geosci. Model Dev.
Discussion started: 6 June 2017

Geoscientific Model Development Discussions

DCMIP2016: A Review of Non-hydrostatic Dynamical Core Design and Intercomparison of Participating Models

Paul A. Ullrich[1], Christiane Jablonowski[2], James Kent[3], Peter H. Lauritzen[4], Ramachandran Nair[4], Kevin A. Reed[5], Colin M. Zarzycki[4], David M. Hall[6], Don Dazlich[7], Ross Heikes[7], Celal Konor[7], David Randall[7], Thomas Dubos[8], Yann Meurdesoif[8], Xi Chen[9], Lucas Harris[9], Christian Kühnlein[10], Vivian Lee[11], Abdessamad Qaddouri[11], Claude Girard[11], Marco Giorgetta[12], Daniel Reinert[13], Joseph Klemp[4], Sang-Hun Park[4], William Skamarock[4], Hiroaki Miura[14], Tomoki Ohno[14], Ryuji Yoshida[15], Robert Walko[16], Alex Reinecke[17], and Kevin Viner[17]

FVM and MPAS results for stratified flow past Schär mountain on a reduced-radius planet after 2 h
(left: potential temperature perturbation θ' [K], right: vertical velocity w [m/s], lon-height section at lat=0)

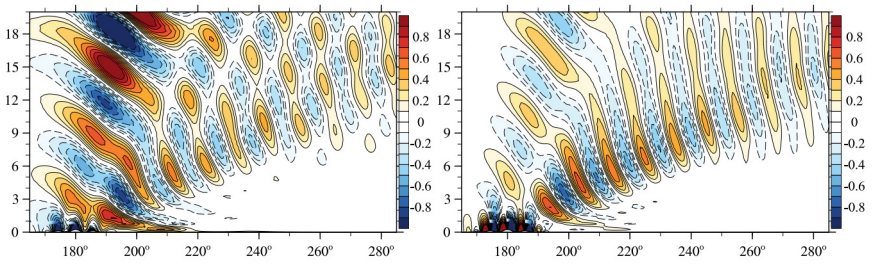

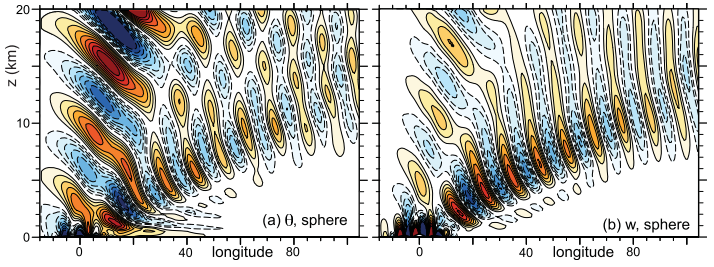

ECMWF

Mesoscale convective storm on reduced-size planet

Supercell evolution (0.5, 1, 1.5, 2h) with FVM (left) and MPAS (right) at ≈ 0.5 km grid spacing (cf. Klemp et al. 2015):

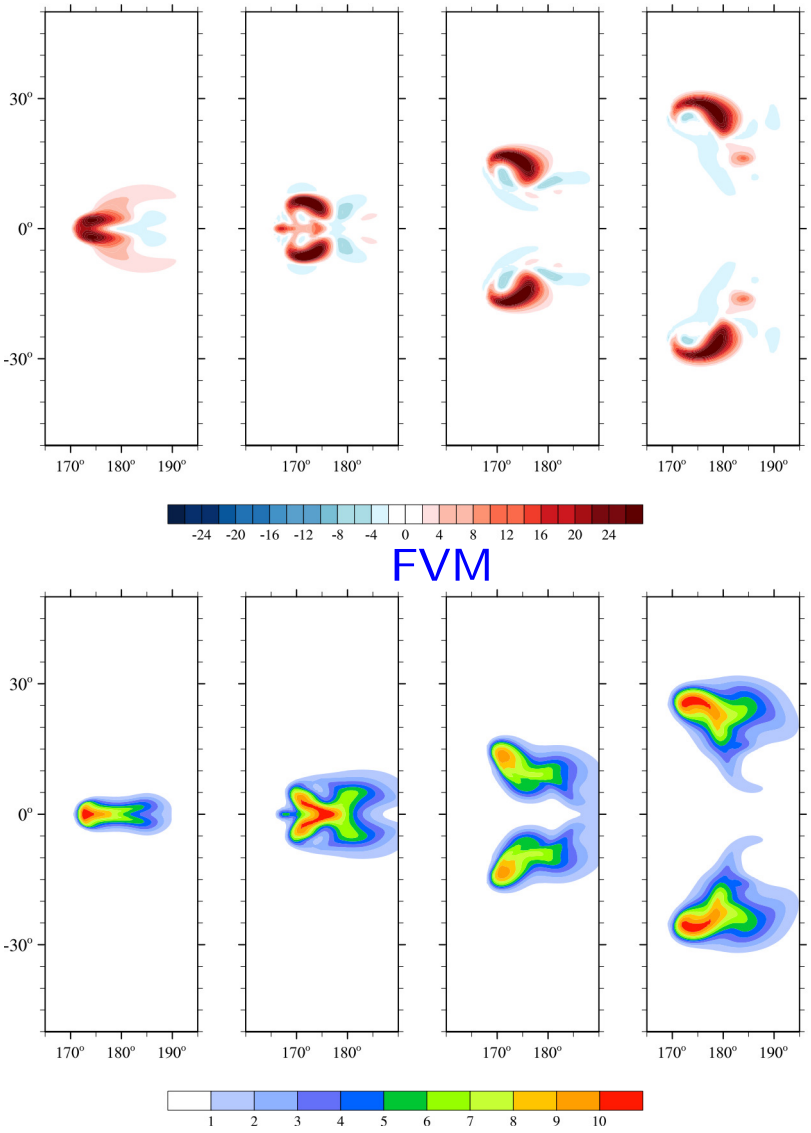

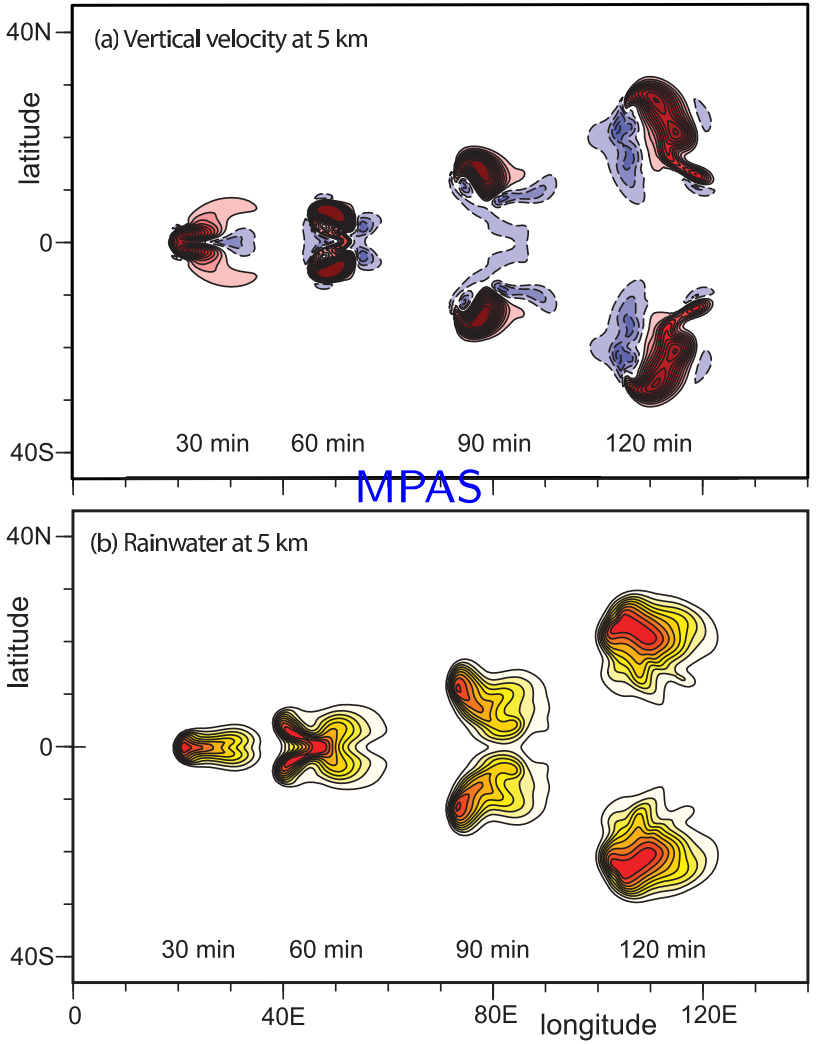

Vertical velocity (m/s) at 5 km

Rainwater (g/kg) at 5 km

Mesoscale convective storm on reduced-size planet

Supercell for grid spacings (4, 2, 1, 0.5 km) with FVM (left) and MPAS (right) after 2 h of simulation (cf. Klemp et al. 2015):

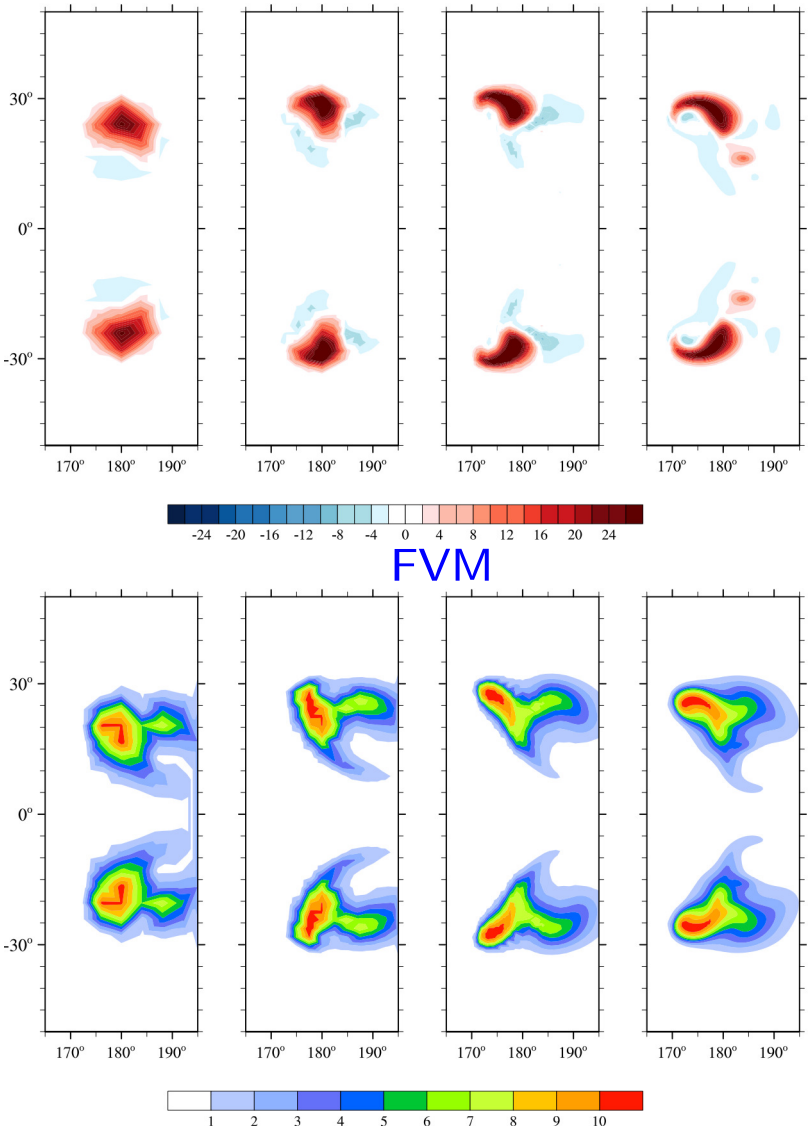

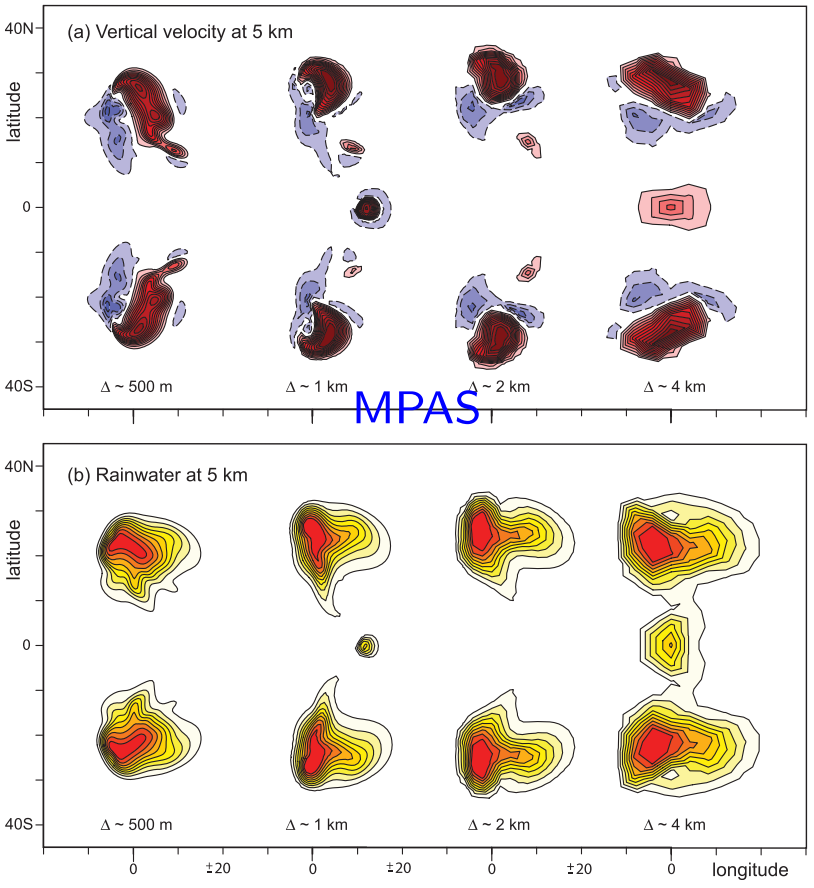

Vertical velocity (m/s) at 5 km

Rainwater (g/kg) at 5 km

Finite-Volume Module references

Further reading:

- Kühnlein C., P. K. Smolarkiewicz, A. Dörnbrack, Modelling atmospheric flows with adaptive moving meshes., J. Comput. Phys., 2012.
- Szmelter J., P. K. Smolarkiewicz P.K, An edge-based unstructured mesh discretisation in a geospherical framework., J. Comput. Phys., 2010.
- Smolarkiewicz P.K., C. Kühnlein, N. P. Wedi, A discrete framework for consistent integrations of soundproof and compressible PDEs of atmospheric dynamics., J. Comput. Phys., 2014.
- Smolarkiewicz P.K., W. Deconinck, M. Hamrud, C. Kühnlein, G. Modzinski, J. Szmelter, N. P. Wedi, A finite-volume module for simulating global all-scale atmospheric flows., J. Comput. Phys., 2016.
- Kühnlein C., Smolarkiewicz P.K., An unstructured-mesh finite-volume MPDATA for compressible atmospheric dynamics., J. Comput. Phys., 2017.
- Smolarkiewicz P.K., C. Kühnlein, W. W. Grabowski, A finite-volume module for cloud-resolving simulations of global all-scale atmospheric flows., J. Comput. Phys., 2017.
- Deconinck W., P. Bauer, M. Diamantakis, M. Hamrud, C. Kühnlein, G. Mengaldo, P. Marciel, T. Quintino, B. Raoult, P. K. Smolarkiewicz, N. P. Wedi, *Atlas*: The ECMWF framework to flexible numerical weather and climate modelling., https://doi.org/10.1016/j.cpc.2017.07.006, 2017.
- Waruszewski M., C. Kühnlein, H. Pawlowska, P. K. Smolarkiewicz, MPDATA: Third-order accuracy for arbitrary flows, *submitted to JCP*
- Kühnlein C., S. Malardel, Smolarkiewicz P.K., Finite-volume and spectral-transform solutions in IFS, *in preparation for GMD*
- Kühnlein C., R. Klein, Smolarkiewicz P.K., Splitting of advection in an all-scale atmospheric model, *in preparation for MWR*

ECMWF